1 General

H-11 Mod is a martensitic hot work die steel which can be heat treated to ultimate strengths up to 300 ksi. It contains chromium, molybdenum, and vanadium to promote hardenability. The alloy is hardened by an austenitizing heat treatment followed by air cooling or oil quenching. Double or triple tempering is employed to achieve the best combinations of strength and toughness. Ultimate tensile strengths of 200 to 300 ksi are developed by appropriate tempering treatments and high strength is maintained at elevated temperatures. H-11 Mod has excellent thermal shock resistance, hot hardness, hot abrasion resistance, and good fatigue properties. The steel has good formability and machinability in the annealed condition, is readily welded, and exhibits little distortion when heat treated. However, the fracture toughness is low and at yield strength levels above 200 ksi care should be taken to avoid small defects if used in critical applications. Concern about the stress corrosion resistance of H-11 Mod fasteners has led to a decrease in use of the alloy in some critical aerospace applications. Wear resistance can be improved by surface treatments such as nitriding. H-11 Mod is widely used in industry for hot work and casting dies, in ordnance for gun barrel and related applications, and in aerospace for landing gear, arrester hooks, solid propellant rocket cases, fasteners, and structural sections.

1.1 Commercial Designation

H-11 Mod

1.2 Alternate Designations

AISI Type H11, SAE Type H11, UNS T20811, Al Tech Potomac A, Carpenter No. 882, Chromo-V, Guterl H-11, Hot Form No. 2.

1.3 Specifications

1.3.1 *[Table]* AMS Specifications.

1.4 Composition

1.4.1 *[Table]* AMS Specified Composition.

1.5 Heat Treatment

1.5.1 General. Heat treatment conditions are critical with regard to developing the desired combination of toughness and strength and preventing quench cracking in H-11 Mod. Good hardenability is conferred in H-11 Mod by the chromium, molybdenum, and vanadium additions, which enable fully or nearly fully martensitic structures to be obtained with modest cooling rates following the initial austenitizing heat treatment. The carbon content of 0.4 percent is required to provide high strength, but also causes a low M_f temperature and high austenite-to-martensite transformation strains. High internal stresses thus can develop if the quench after austenitizing is severe, especially in large sections. Air cooling with or without forced circulation is appropriate under most circumstances.

Fe
0.4 C
5.0 Cr
1.3 Mo
0.5 V

The most stable carbide in H-11 Mod is VC, which is only partially dissolved at an austenitizing temperature of 1900F. Other carbides, such as Mo_2C containing dissolved chromium and vanadium and chromium-molybdenum-rich $M_{23}C_6$, are also present. These undissolved carbides particles pin the grain boundaries and help maintain the highly desirable fine austenite grain size. As the carbides dissolve with increasing austenitizing temperature, the carbon content of the austenite increases and the subsequent martensite phase is progressively hardened. The optimum austenitizing temperature thus represents in part a balance between maintenance of a fine austenite grain size and hardness of the martensite phase.

Double tempering is required in order to develop full toughness, especially in larger sections. The first tempering treatment causes any retained austenite to transform to a ferrite-carbide aggregate such as bainite or to precipitate alloy carbides, which raises the M_f temperature so that the retained austenite transforms to martensite on cooling. This new martensite is then tempered during the second tempering treatment. At least two and in some cases three or more tempering treatments are recommended to minimize retained austenite and untempered martensite. Retained austenite is particularly undesirable as it can transform during service and cause distortion or cracking.

H-11 Mod is a "secondary hardening" steel, i.e., room temperature hardness increases with increasing tempering temperature up to the temperature of maximum secondary hardening, about 950F. Secondary hardening is associated with reprecipitation of VC in which some molybdenum is dissolved. At higher tempering temperatures, overageing occurs with coarsening of the VC and additional precipitation of $M_{23}C_6$. Increased austenitizing temperature, in addition to increasing the carbon content of the martensite, increases the extent of the secondary hardening reactions. Maintenance of properties at high operating temperatures is promoted by these secondary hardening reactions.

Alternative explanations for the reactions responsible for secondary hardening have been advanced, as discussed in Section 3.2.3.6. Also the data on relative carbide abundance after tempering, presented later in Figure 2.1.2.4, do not indicate a major role for VC, in disagreement with the reactions suggested in the previous paragraph.

Tempering at the temperature of maximum secondary hardening is not recommended due to the marked embrittlement which occurs. The optimum tempering temperature for this steel is about 1100F.

1.5.2 Normalize. Generally not necessary. For effective homogenization, heat to about 1950F, soak 1 hour for each inch of thickness, and air cool. Anneal immediately after the part reaches room temperature. There is a possibility that H-11 Mod may crack during this treatment.

1.5.3 Anneal. Heat to 1550 to 1625F and hold to equalize temperature, cool slowly in the furnace to about 900F, then more rapidly to room temperature. This treatment should produce a fully spheroidized microstructure free of grain boundary carbide networks.

1.5.4 Austenitize. Preheat to 1400 to 1500F and then raise the temperature to 1850 to 1875F and hold 20 min plus 5 min for each 1 inch of thickness, air cool. For section thicknesses greater than 10 inches, austenitize at 1825-1850F and oil quench. For parts with abrupt section changes, quench in salt bath to 800F, hold for 20 to 30 minutes to equilibrate, then air cool to room temperature.

1.5.5 Temper. Heat at 950 to 1200F, depending on strength desired. Close temperature control is important, since properties change sharply with temperature. Double temper, 1 to 4 hours each, depending on thickness, and cool to room temperature between tempers. Triple tempering is more desirable, especially for critical parts. For high temperature applications, parts should be tempered at a temperature above the maximum service temperature to guard against undesirable property changes during service. Distortion during tempering is very low, not exceeding 0.001 inch per inch of cross-section.

1.5.6 Intermediate Anneal. Heat to 1200 to 1250F, 4 hours, air cool. This treatment is used to achieve greater dimensional accuracy in heat treated parts by intermediate annealing rough-machined parts, then finish machining, and finally heat treating to the desired hardness.

1.5.7 Stress Relief. Heat at 875 to 900F, 2 to 4 hours, for finished parts after grinding, machining, or straightening (Refs. 81, pp. 439-441; Refs. 82-86; Ref. 98, pp. 8-11).

1.6 Hardness

1.6.1 *[Figure]* End quench hardenability.

1.6.2 *[Figure]* Effect of austenitizing temperature and type of cooling on hardness.

1.6.3 *[Figure]* Effect of carbon content and tempering temperature on hardness of air melt and vacuum melt alloy.

1.6.4 *[Figure]* Effect of austenitizing temperature and tempering temperature on hardness for a single tempering treatment.

1.6.5 *[Figure]* Effect of austenitizing temperature and tempering temperature on hardness for a double tempering treatment.

1.6.6 *[Figure]* Effect of austenitizing temperature and tempering temperature on hardness for a triple tempering treatment.

1.6.7 *[Figure]* Effect of low temperature on hardness of sheet.

1.6.8 *[Figure]* Hot hardness of bar austenitized at 1825 or 1900F and tempered at temperatures from 1025 to 1225F.

1.6.9 *[Figure]* Hot hardness after tempering at 1050 to 1150F.

1.7 Forms and Conditions Available

1.7.1 H-11 Mod is available in the form of forgings, extrusions, billets, plate, sheet, strip, bar, rod, and wire.

1.8 Melting and Casting Practice

1.8.1 Standard practice includes electric furnace air melting, induction vacuum, and consumable electrode vacuum melting. Vacuum arc remelting, vacuum degassing, and electroslag refining are effective in producing cleaner, finer-grained, and more uniform alloy with greater freedom from segregation and harmful impurities and with improved toughness.

1.9 Special Considerations

1.9.1 Decarburization can occur during heat treatment unless special precautions are taken. Heat treatments should be conducted in a neutral atmosphere furnace or salt bath or with parts packed in a neutral packing compound.

1.9.2 Parts should be protected from hydrogen embrittlement by baking for a minimum of 24 hours at 375F or higher after plating in an acid bath or after other processing that might introduce hydrogen into the metal.

1.9.3 Sulfur adversely affects notch impact strength and should be held low, preferably below 0.005 percent.

1.9.4 Alloy has low fracture toughness after tempering at 1000F to high strength levels. However, the fracture toughness can be improved at a cost of decreased strength by increasing the tempering temperature above 1000F, the approximate temperature of maximum secondary hardening

2 Physical Properties and Chemical Environmental Effects

2.1 Thermal Properties

2.1.1 Melting Range, 2500-2600F (Ref. 23, p. 22).

2.1.2 Phase Changes.

2.1.2.1 *[Figure]* Time-temperature-transformation diagram.

2.1.2.2 The TTT diagram for transformation of austenite to pearlite exhibits the usual C curve with the nose temperature at 1330F and the bay temperature inferred to be approximately 1200F, as shown in Figure 2.1.2.1.

The rate of transformation to pearlite can be markedly accelerated by pre-deforming the austenitic alloy at 1200F. This acceleration is related to an increase in the pearlite nucleation rate per unit volume of material (Ref. 87, p. 776).

2.1.2.3 The A_{c1} transformation temperature from ferrite to austenite on heating is 1505-1580F. The A_{r1} temperature on cooling is 1490-1445F.

2.1.2.4 *[Figure]* Relative carbide intensity (abundance) as a function of tempering temperature.

2.1.3 Thermal Conductivity.

2.1.3.1 *[Figure]* Thermal Conductivity.

2.1.4 Thermal Expansion.

2.1.4.1 *[Figure]* Thermal Expansion.

2.1.5 Specific Heat, 0.11 Btu per lb F.

2.1.6 Thermal Diffusivity.

2.2 Other Physical Properties

2.2.1 Density, 0.280 lb per cu. in. 7.75 gr per cu. cm.

2.2.2 Electrical Properties.

2.2.2.1 *[Figure]* Electrical resistivity.

2.2.3 Magnetic Properties. This steel is highly ferro-magnetic, but becomes nonmagnetic at temperatures above 1400 to 1500F.

2.2.4 Emittance.

2.2.4.1 *[Figure]* Emittance.

2.2.5 Damping Capacity.

2.3 Chemical Environments

2.3.1 General Corrosion. The general corrosion resistance of this steel is low and surface protection is required.

2.3.2 Stress Corrosion.

2.3.2.1 H-11 Mod has good stress-corrosion resistance as compared to other non-stainless steels heat treated to comparable strength levels, as shown in Figure 2.3.2.2. The good stress-corrosion resistance of H-11 Mod may be due to its combination of high chromium and molybdenum contents. Higher purity vacuum melted material and material final tempered at higher temperatures have improved stress-corrosion resistance, as shown in Figures 2.3.2.3, 2.3.2.4, and 2.3.2.5. The stress-corrosion resistance in an aqueous solution of NaCl is similar to that in distilled water, as shown in Figure 2.3.2.6.

The threshold stress intensity for stress-corrosion cracking is much less than the fracture toughness when tested in seacoast environments or aqueous salt solutions (Tables 2.3.2.7 and 2.3.2.8). Similarly the crack growth rate is greatly increased in distilled water and in moist argon as compared to dry argon (Figures 2.3.2.9 and 2.3.2.10).

2.3.2.2 *[Figure]* Comparison of stress-corrosion cracking characteristics of alloy with corresponding behavior of several other martensitic steels heat treated to tensile strength levels of approximately 240 ksi.

2.3.2.3 *[Figure]* Effect of applied stress on time to stress-corrosion failure for air-melt and vacuum melt alloy.

2.3.2.4 *[Figure]* Effect of temperature of final temper on stress-corrosion resistance in 5 percent aqueous solution of NaCl.

2.3.2.5 *[Figure]* Effect of tempering temperature on stress-corrosion resistance of billet.

2.3.2.6 *[Figure]* Delayed failure of alloy at 206 ksi yield strength level when tested in distilled water and in aqueous solution containing 3 percent NaCl.

2.3.2.7 *[Table]* Plane strain fracture toughness and threshold for stress-corrosion cracking in seacoast test and in accelerated tests for alloy in three conditions.

2.3.2.8 *[Table]* Plane strain fracture toughness and threshold for stress-corrosion cracking in 3-1/2 percent NaCl aqueous solution.

2.3.2.9 *[Figure]* Sustained load crack growth rate in humid argon and in distilled water.

2.3.2.10 *[Figure]* Effect of stress intensity on crack growth rate for a wide range of relative humidity in an argon environment.

2.3.2.11 In the heat treated condition for F_{ty} = 245 ksi, alloy is susceptible to severe rusting (accompanying stress-corrosion cracking) when subjected to a moist chloride environment or a semi-industrial atmosphere (Ref. 50, p. 4).

2.3.2.12 H-11 Mod double tempered at 970 or 1100F is not subject to stress corrosion when exposed in hydraulic oil (Ref. 89, pp. 347-353).

2.3.2.13 Pitting and stress corrosion can result from use of manufacturing chemicals high in sulfur or chlorine. These chemicals include cutting fluids, penetrating fluids, solvents, lubricants and penetrants, developers, anti-seize thread compounds, steam cleaners, and machining coolants. Sulfur and chlorine contents of these fluids should be held below 5500 ppm each to minimize the possibility of stress corrosion. The addition of thermally stable corrosion inhibitors such as triethanolamine reduces the corrosivity of these chemicals (Ref. 90, pp. 59-65).

2.3.3 Hydrogen Embrittlement.

2.3.3.1 Hydrogen embrittlement may occur in material heat treated to high strength if exposed to a hydrogen-containing environment. Certain surface treatments such as acid or alkaline pickling, cathodic cleaning, or phosphatizing

may result in hydrogen embrittlement for material having F_{tu} of 200 ksi or higher. Approved plating methods should be followed by baking at temperatures ranging from 375F for 23 hours to 950F for short times (Ref. 57, p. 127).

2.3.3.2 Acid baths used in chemical milling initially embrittle alloy, but recovery of ductility occurs within one week at RT if there is no barrier to escape of hydrogen (such as plating). A recovery treatment of 48 hours at RT followed by 4 hours at 375F is recommended (Ref. 76).

2.3.3.3 *[Table]* Notch strength in helium and hydrogen at 10 ksi pressure.

2.3.3.4 The diffusivity of hydrogen in H-11 Mod at 72F is 3×10^{-8} cm^2/sec. (Ref. 91, p. 437).

2.4 Nuclear Environments

2.4.1 H-11 Mod has good resistance to swelling following high fluence neutron irradiation. As shown in Figure 2.4.2, swelling in H-11 Mod ranges from -0.3 to +0.16 percent under the indicated conditions, slightly less than observed for Type 416 martensitic stainless steel. By comparison, 20 percent cold-worked Type 316 austenitic stainless steel would be expected to swell about 30 percent at its peak swelling temperature of 1100F. H-11 Mod shows promise for fusion reactor first wall applications in terms of swelling resistance (Ref. 92, pp. 969-973).

2.4.2 *[Figure]* Effect of irradiation temperature on swelling in H-11 Mod and Type 416 Martensitic Stainless Steel.

3 Mechanical Properties

3.1 Specified Mechanical Properties

3.1.1 *[Table]* AMS specified mechanical properties.

3.2 Mechanical Properties at Room Temperature

3.2.1 Tension Stress-strain Diagrams and Tensile Properties.

3.2.1.1 Stress-strain relations.

3.2.1.1.1 *[Figure]* Stress-strain curves for bar tempered at 950 to 1300F.

3.2.1.2 Heat treatment effects. This next group of figures illustrates primarily the effects of tempering temperature on tensile properties. Of particular interest is the steepness of the decrease in tensile strength with increasing tempering temperature for tempering temperatures above 1000F (Figures 3.2.1.2.1 and 3.2.1.2.2), emphasizing the need for strict temperature control during tempering. Also of interest is the secondary hardening peak at 950F, most apparent in Figure 3.2.1.2.2. Transverse tensile properties are similar to longitudinal tensile properties (Figure 3.2.1.2.3). Increased carbon content increases the tensile strength of hardened and tempered alloy, while vacuum melting results in improved tensile ductility (Figure 3.2.1.2.4).

3.2.1.2.1 *[Figure]* Effects of tempering at 900 to 1300F on tensile properties of sheet and bar.

3.2.1.2.2 *[Figure]* Effects of tempering up to 1300F on tensile properties of bar.

3.2.1.2.3 *[Figure]* Effects of tempering at 1000 to 1100F on transverse tensile properties of bar and extrusion.

3.2.1.2.4 *[Figure]* Effects of carbon content and tempering temperature on tensile properties of air melted and vacuum melted alloy.

3.2.1.3 Exposure effects. Exposure at temperatures of -300F and lower results in increased strength and decreased ductility on subsequent room temperature testing, shown in Figure 3.2.1.3.1. This behavior may result from additional austenite-to-martensite transformation. The approximate high temperature time-temperature limits for stability of mechanical properties are shown in Figure 3.2.1.3.2.

3.2.1.3.1 *[Figure]* Effects of low temperature exposure on tensile properties of sheet.

3.2.1.3.2 *[Figure]* Maximum temperatures for stability of mechanical properties for various exposure times.

3.2.1.4 Thermomechanical processing effects. Deformation during or after heat treatment increases strength and slightly decreases ductility. The effects of warm rolling after austenitizing (ausforming) on the properties of untempered alloy are shown in Figure 3.2.1.4.1. Tempering after ausforming reduces strength and improves ductility similarly to conventional austenitized and tempered alloy but the strength improvements from ausforming are retained, as shown in Figures 3.2.1.4.2, 3.2.1.4.3, and 3.2.1.4.4. Strength increases are also effected by prestraining and aging material which has been previously austenitized and tempered, shown in Figure 3.2.1.4.5.

3.2.1.4.1 *[Figure]* Effects of rolling on tensile properties of austenitized sheet.

3.2.1.4.2 *[Figure]* Effects of forging and tempering on tensile properties of austenitized steel.

3.2.1.4.3 *[Figure]* Effects of forging and tempering on tensile properties of vacuum melted alloy.

3.2.1.4.4 *[Figure]* Effects of tempering temperature on yield strength for conventional alloy and ausformed alloy.

3.2.1.4.5 *[Figure]* Effects of pre-straining on tensile properties of austenitized and tempered sheet.

3.2.1.5 Environmental effects.

3.2.1.5.1 *[Table]* Tensile properties of bar in air at atmospheric pressure and in helium and hydrogen at 10 ksi pressure.

3.2.2 Compression Stress-strain Diagrams and Compression Properties.

3.2.2.1 *[Figure]* True stress - true strain curves in tension and compression of bar.

3.2.2.2 *[Figure]* True stress - true strain curves in tension and compression for ausformed bar.

3.2.3 Impact.

3.2.3.1 The impact energy of H-11 Mod decreases with increasing tempering temperature to a minimum at about 900F, then increases with further increases in tempering temperature, shown in Figures 3.2.3.2 - 3.2.3.5. This behavior is a further reflection of the secondary hardening reaction shown earlier to affect tensile properties. The detrimental effects of increasing carbon content and the beneficial effects of vacuum melting on impact energy are also illustrated in Figure 3.2.3.4.

3.2.3.2 *[Figure]* Effect of tempering temperature on Charpy impact energy at RT and -321F.

3.2.3.3 *[Figure]* Effects of tempering temperature on Charpy impact energy and hardness.

3.2.3.4 *[Figure]* Effect of carbon content and tempering temperature on Charpy impact strength of air melt and vacuum melt alloy.

3.2.3.5 *[Figure]* Effect of tempering temperature on tensile and yield strength and on Izod impact energy.

3.2.3.6 Several possible causes have been advanced for the secondary hardening behavior exhibited by H-11 Mod. One possible cause involves the carbide precipitation reactions discussed earlier in Section 1.5.1. A second possibility relates to alloy composition. As shown in Figure 3.2.3.7, both commercial H-11 Mod and a laboratory heat containing zero manganese showed decreased impact energy after tempering at 932 or 1022F. However, a second laboratory heat with both manganese and silicon removed did not exhibit embrittlement, suggesting that embrittlement may be associated with silicon content. A third possible cause for embrittlement is suggested by a study of the effects of both time and temperature of retempering on impact energy, the results of which are shown in Figure 3.2.3.8. Kinetic data derived from this figure, along with additional microstructural and microchemical observations (Ref. 93, p. 1182), suggest that segregation primarily of phosphorus but also of sulfur and silicon to preaustenitic grain boundaries and other interfaces may be responsible for secondary embrittlement.

3.2.3.7 *[Figure]* Effects of tempering temperature and manganese and silicon contents on Charpy impact energy.

3.2.3.8 *[Figure]* Effects of retempering time and temperature on Charpy impact energy and hardness.

3.2.4 Bending.

3.2.5 Torsion and Shear.

3.2.6 Bearing.

3.2.6.1 *[Table]* Typical bearing and shear properties.

3.2.7 Stress Concentration.

3.2.7.1 Notched properties, see also Sections 3.3.7 and 3.5.

3.2.7.1.1 Material tempered at 900 to 1050F is particularly notch-sensitive. However, the notch-sensitivity decreases with increasing tempering temperature and is essentially absent for material tempered at 1200F, as shown in Figures 3.2.7.1.2 and 3.2.7.1.3. Increasing stress concentration factor and increasing length of initial fatigue crack both sharply reduce the notch strength of material tempered at 1000 or 1060F, but less strength reduction is noted for material tempered at 1100 or 1150F (Figures 3.2.7.1.4 and 3.2.7.1.5). Increased carbon content is beneficial to notch strength. As illustrated in Figure 3.2.7.1.6, for a given original ultimate strength, the notch strength increases with increasing carbon content.

3.2.7.1.2 *[Figure]* Effects of tempering temperature on notch strength of sharply notched sheet.

3.2.7.1.3 *[Figure]* Effects of tempering temperature on sharp notch strength ratio for sheet.

3.2.7.1.4 *[Figure]* Effects of stress concentration on notch strength of heat treated sheet.

3.2.7.1.5 *[Figure]* Effects of initial crack length on net section strength for sheet heat treated to F_{tu} from 200 to 300 ksi.

3.2.7.1.6 *[Figure]* Effect of carbon content and strength on sharp edge notch tensile strength ratio of air melt and vacuum melt sheet.

3.2.7.2 Fracture toughness.

3.2.7.2.1 Increasing austenizing temperature decreases the fracture toughness for material subsequently tempered to medium strength-high toughness at 1202F but not for material tempered to high strength-lower toughness at 1022F. Also, decreasing the volume percent of microstructural inclusions by argon ladling increases the fracture toughness of the 1202F-tempered material but not of the 1022F-tempered material, as shown in Figure 3.2.7.2.2. Tempering temperature significantly affects fracture toughness. A minimum in fracture toughness is observed for a tempering temperature of 1000F, the temperature region of maximum secondary hardening, as shown in Figure 3.2.7.1.2. (Additional fracture toughness data in Tables 2.3.2.7 and 2.3.2.8 support the trends shown in Figure 3.2.7.2.3.)

3.2.7.2.2 *[Figure]* Effects of austenitizing temperature, tempering temperature, and melting practice on fracture toughness.

3.2.7.2.3 *[Figure]* Effect of tempering temperature on fracture toughness.

3.2.8 Combined Properties.

3.3 Mechanical Properties at Various Temperatures

3.3.1 Tension Stress-strain Diagrams and Tensile Properties.

3.3.1.1 *[Figure]* Stress-strain curves at room and low temperatures for sheet.

3.3.1.2 *[Figure]* Stress-strain curves at room and elevated temperatures for materials heat treated to F_{tu} = 260 ksi.

3.3.1.3 *[Figure]* Stress-strain curves at room and elevated temperatures for annealed sheet.

3.3.1.4 *[Figure]* Stress-strain curves at room and elevated temperatures for sheet heat treated to F_{tu} = 280 ksi.

3.3.1.5 *[Figure]* Stress-strain curves at room and low temperatures for bar.

3.3.1.6 *[Figure]* Effect of low test temperature on tensile properties of bar.

3.3.1.7 *[Figure]* Effect of low test temperature on tensile properties of sheet.

3.3.1.8 *[Figure]* Effect of test temperature on tensile properties for tempering temperatures of 1000F to 1150F of bar and sheet.

3.3.1.9 *[Figure]* Effects of test temperature and tempering temperature on tensile properties of bar.

3.3.1.10 *[Figure]* Effect of test temperature on tensile properties of bolts heat treated to F_{tu} = 220 ksi minimum.

3.3.1.11 *[Figure]* Effects of test temperature, holding time and strain rate on tensile properties of sheet.

3.3.1.12 *[Figure]* Effect of test temperature on tensile properties of air melt alloy tempered to F_{tu} = 260 ksi and 310 ksi.

3.3.1.13 *[Figure]* Effects of test temperature on tensile properties of ausformed and conventionally heat treated steel.

3.3.1.14 *[Figure]* Effect of test temperature on tensile properties of annealed sheet.

3.3.1.15 *[Figure]* Effect of elastic strain rate on yield stress at RT and 600F.

3.3.1.16 *[Figure]* Effect of test temperature on tensile properties of sheet heat treated to F_{tu} = 260 and 280 ksi minimum.

3.3.2 Compression Stress-strain Diagrams and Compression Properties.

3.3.2.1 *[Figure]* Stress-strain curves in compression at room and elevated temperatures for annealed sheet.

3.3.2.2 *[Figure]* Effect of test temperature on compressive yield strength of sheet.

3.3.2.3 *[Figure]* Effect of test temperature on compressive yield strength of annealed sheet.

3.3.3 Impact.

3.3.3.1 *[Figure]* Effect of temperature on Charpy impact energy of bar.

3.3.3.2 *[Figure]* Effect of carbon content and test temperature on Charpy impact strength of air melt and vacuum melt alloy.

3.3.4 Bending.

3.3.5 Torsion and Shear.

3.3.5.1 *[Figure]* Effect of test temperature on shear strength of heat treated bolts.

3.3.5.2 *[Figure]* Effect of test temperature on shear strength of annealed sheet.

3.3.6 Bearing.

3.3.6.1 *[Figure]* Effect of test temperature on bearing properties of annealed sheet.

3.3.7 Stress Concentration.

3.3.7.1 Notch properties.

3.3.7.1.1 *[Figure]* Effect of test temperature on notch strength for various stress concentration factors of sheet.

3.3.7.1.2 *[Figure]* Effect of low test temperature on notch strength of sheet.

3.3.7.1.3 *[Figure]* Effect of low test temperature on notch tensile strength for stress concentration factors from 4 to 12.5.

3.3.7.1.4 *[Figure]* Effect of low temperatures, loading rates and stress concentration factors on notch strength of sheet.

3.3.7.1.5 *[Figure]* Effects of low test temperature and tempering temperature on notch strength of bar.

3.3.7.1.6 *[Figure]* Effects of low test temperature on crack strength of sheet.

3.3.7.1.7 *[Figure]* Effects of low test temperature and tempering temperature on crack strength of bar.

3.3.7.1.8 *[Figure]* Effect of test temperature on crack strength of sheet.

3.3.7.2 Fracture toughness.

3.3.7.2.1 *[Figure]* Effect of test temperature on smooth specimen tensile properties and on fracture toughness of plate.

3.4 Creep and Creep Rupture Properties

3.4.1 *[Figure]* Creep rupture behavior at 900 to 1200F for two tempering temperatures.

3.4.2 *[Figure]* Creep rupture curves for alloy at various strength levels at 700 to 1000F.

3.4.3 *[Figure]* Creep rupture curves at 800 to 1000F for sheet heat treated to F_{tu} = 190 ksi.

3.4.4 *[Figure]* Short time creep and creep rupture curves at 1000 and 1200F for sheet heat treated to F_{tu} = 290 ksi.

3.4.5 *[Figure]* Stress to produce creep rates of 10^{-3} to 10^{-5} percent per hour at 700 to 900F.

3.5 Fatigue Properties

3.5.1 Conventional Fatigue.

3.5.1.1 *[Figure]* S-N curves for heat treated bar.

3.5.1.2 *[Figure]* Fatigue scatterband for bar specimens from eight separate heats tested in axial tension.

3.5.1.3 *[Figure]* S-N curves for notched and smooth specimens at room temperature.

3.5.1.4 *[Figure]* S-N curves for notched and smooth specimens at 800F.

3.5.1.5 *[Figure]* S-N curves for notched and smooth specimens at 1000F.

3.5.1.6 *[Table]* Fatigue properties of bar and bolts.

3.5.1.7 *[Table]* Tensile and fatigue properties at room temperature and at -320F for bolts machined from bar heat treated to 240 ksi yield strength.

3.5.1.8 *[Table]* Tensile and fatigue properties of bolts made from material heat treated to several strength levels.

3.5.1.9 *[Figure]* Low-cycle fatigue of notched (K_t = 5.0) specimens cut from large plate.

3.5.1.10 *[Figure]* Low-cycle fatigue of notched (K_t = 3.0) specimens cut from long and short transverse directions of forging.

3.5.1.11 *[Figure]* Effect of surface machining and grinding (to remove decarburized layer) on reversed bending fatigue of sheet.

3.5.1.12 *[Table]* Fatigue strength at 10^6 cycles in rotating bending for vacuum and air melted alloy in various conditions of surface treatment after exposure to elevated temperature.

3.5.1.13 *[Figure]* S-N curves in rotating beam bending for smooth specimens and for specimens subjected to glass bead peening.

3.5.1.14 *[Figure]* Cyclic strain hardening in ausformed bar as manifested by reduction in plastic strain range (increase in elastic strain range) as cycles are increased during strain cycling tests in which total strain amplitudes are maintained constant.

3.5.1.15 *[Figure]* S-N curves for ausformed and conventionally heat treated steel.

3.5.2 Fatigue Crack Propagation.

3.5.2.1 The threshold stress intensity for fatigue crack propagation is considerably less than the plane strain fracture toughness and varies inversely with stress ratio R, as seen in Figure 3.5.1.2. This behavior is observed also with other high strength martensitic steels. The exponent "m" in the relation

$$da/dn = C\Delta K^m$$

is about 3 for H-11 Mod, compared to a range of 2.3 to 3.1 for other steels such as Type 4340, Hy-Tuf, and A-286.

3.5.2.2 *[Figure]* Fatigue crack growth rates in air at room temperature.

3.5.2.3 *[Figure]* Fatigue crack growth rates in air at 650F.

3.6 Elastic Properties

3.6.1 Poisson's Ratio, 0.281.

3.6.2 Modulus of Elasticity.

3.6.2.1 *[Figure]* Modulus of elasticity at room and elevated temperature.

3.6.2.2 *[Figure]* Modulus of elasticity for alloy heat treated to various hardness levels.

3.6.2.3 *[Figure]* Modulus of elasticity in compression at room and elevated temperatures for annealed sheet.

3.6.3 Modulus of Rigidity.

3.6.4 Tangent Modulus.

3.6.4.1 *[Figure]* Tangent modulus curves at room and elevated temperatures for bar heat treated to F_{tu} = 260 ksi.

3.6.5 Secant Modulus.

4 Fabrication

4.1 Forming

4.1.1 General. This alloy, in the fully annealed condition, can be readily formed by all common methods.

4.1.2 Forging. H-11 Mod is readily forged at temperatures in the range 1950 to 2100F. Forging stock should be preheated at 1500F to insure temperature uniformity, then slowly further heated to the forging temperature. Forging should not be continued below 1700F, but parts may be reheated as often as necessary. Care must be exercised during cooling after forging to prevent stress cracking. Small simple forgings may be cooled slowly in lime or dry ashes, but larger parts should be soaked at 1450F after forging and furnace cooled. Forged parts should then be annealed as soon as possible.

4.1.3 Bending. Sheet with thickness less than 0.090 inch has a room temperature production bend factor of 2 in the annealed condition and 6 when heat treated to F_{tu} = 260 to 280 ksi.

4.1.4 Straightening can be performed either during cooling from austenitizing or during heating for tempering.

4.2 Machining and Grinding

4.2.1 H-11 Mod is readily machinable in the annealed condition. It has a machinability rating of 55-75 compared to 100 for a 1 percent carbon tool steel or about 40-50 compared to 100 for B1112. Stress corrosion may result from the use of cutting fluids or cleaning fluids high in sulfur or chlorine (see Figure 2.3.2.9). Hydrogen embrittlement may occur during chemical milling (see Section 2.3.3.2).

4.3 Joining

4.3.1 Fusion welding is accomplished using inert gas shielding or with coated electrodes. Filler metal should be of the same general composition as the base metal. Parts to be welded should be preheated to 1000F and temperature should be maintained above 600F during welding. Welded parts, especially those with heavy sections, should be cooled slowly in a furnace or in an insulating medium after welding to prevent cracking. Welded parts should then be given a full anneal as soon after welding as possible. Welding should be performed in the annealed condition. However, if welding is performed in the hardened condition, the part must be retempered after welding. Maximum strength in welded tanks may be obtained after an intermediate temper at 1050F, as shown in Figure 4.3.2. These data further show significantly lower strengths for vessels welded from material previously tempered at 950 or 1000F, suggesting that tempering temperatures of 1050F or higher are preferable for material to be welded.

4.3.2 *[Figure]* Effect of tempering temperature on strength of welded sheet and pressure vessels.

4.4 Surface Treating

4.4.1 Conditions having higher strength than 200 ksi should be cleaned by mechanical methods or by anodic pickling. Acid or alkaline pickling or cathodic cleaning can result in hydrogen embrittlement.

4.4.2 Corrosion and oxidation resistance of this steel is obtained by a variety of surface coatings. One preferred method is plating with nickel cadmium (AMS 2416). (Ref. 101) Aluminizing, chromizing, vapor deposition of metal coatings, and silicone paints are also successfully used in production. Special plating methods are used for the high strength conditions, usually followed by baking at 375F minimum, for 23 hours.

4.4.3 Chemical milling may be accomplished in either the annealed or heat treated conditions. Baking of heat treated parts after chemical milling is recommended. The mechanical properties of sheet heat treated to F_{tu} = 280 ksi minimum and milled from 0.200 to 0.100 in thickness were found to be unchanged.

4.4.4 The surface of H-11 Mod can be hardened using either conventional nitriding or ion nitriding techniques. Temperatures employed are frequently in the range 1000 to 1100F in order to obtain the best efficiency and yet avoid formation of the epsilon-prime iron nitride phase, which flakes off easily. Ion nitriding can be accomplished at temperatures as low as 300F. Nitrogen and hardness profiles for H-11 Mod ion nitrided at 480F are shown in Figure 4.4.5. The calculated diffusivity of nitrogen in H-11 Mod at this temperature is 1.74×10^{-10} cm^2/sec. (Ref. 99, p. 1495).

4.4.5 *[Figure]* Nitrogen content and hardness profiles for ion-nitrided H-11 Mod.

Table 1.3.1 AMS Specifications (Refs. 77-80)

Alloy: H-11 Mod	
AMS Specification	**Product Form**
6437D	Sheet, Strip, and Plate
6485F	Bars, Forgings, and Forging Stock
6487F	Bars, Forgings, and Forging Stock (premium quality, consumable electrode vacuum melted)
6488C	Bars, Forgings, and Forging Stock (premium quality)

Table 1.4.1 AMS Specified Composition (Refs. 77-80)

Alloy: H-11 Mod		
Element	**Percent**	
	Min	**Max**
Carbon	0.38	0.43
Chromium	4.75	5.25
Molybdenum	1.20	1.40
Vanadium	0.40	0.60
Silicon	0.80	1.00
Manganese	0.20	0.40
Copper	-	0.35
Nickel	-	0.25
Phosphorus	-	0.020 (a)
Sulfur	-	0.020 (a)
Iron	Balance	

(a) Max phosphorus and sulfur contents are 0.015 percent for AMS 6487F and AMS 6488D.

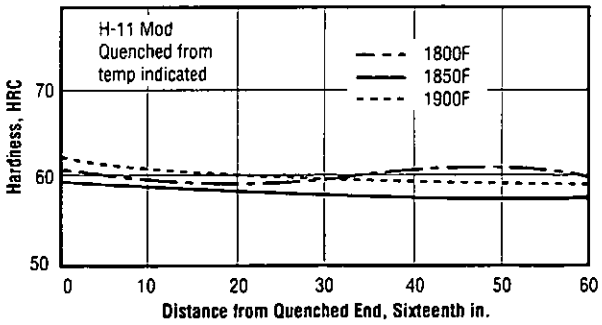

Fig. 1.6.1 End quench hardenability (Ref. 9)

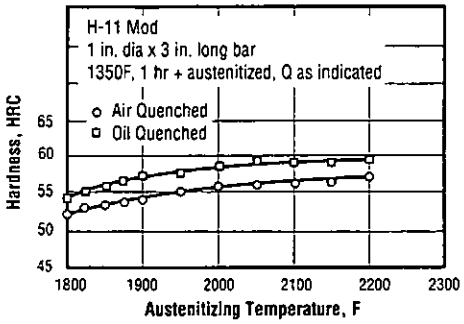

Fig. 1.6.2 Effect of austenitizing temperature and type of cooling on hardness (Ref. 82)

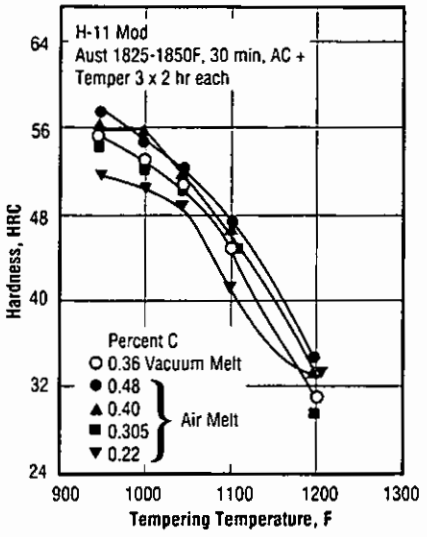

Fig. 1.6.3 Effect of carbon content and tempering temperature on hardness of air melt and vacuum melt alloy (Ref. 22)

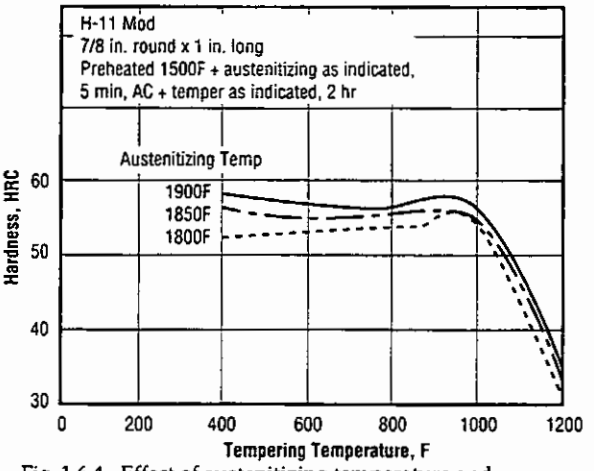

Fig. 1.6.4 Effect of austenitizing temperature and tempering temperature on hardness for a single tempering treatment (Ref. 38)

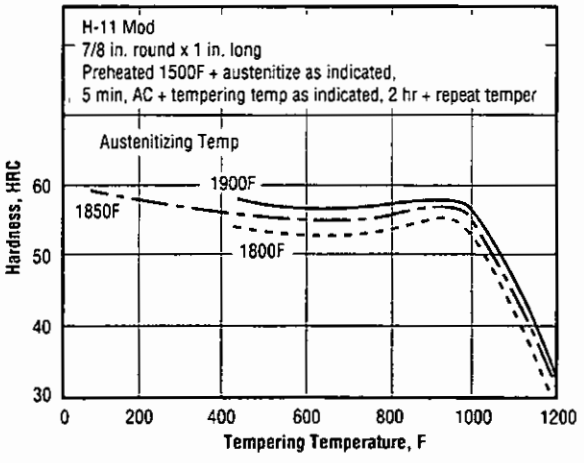

Fig. 1.6.5 Effect of austenitizng temperature and tempering temperature on hardness for a double tempering treatment (Ref. 38)

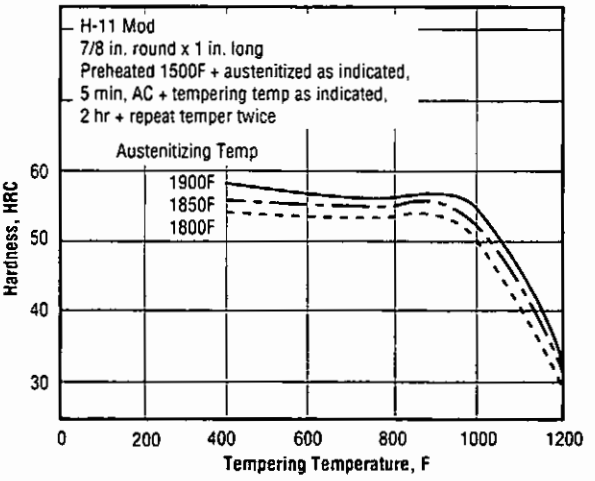

Fig. 1.6.6 Effect of austenitizing temperature and tempering temperature on hardness for a triple tempering treatment (Ref. 38)

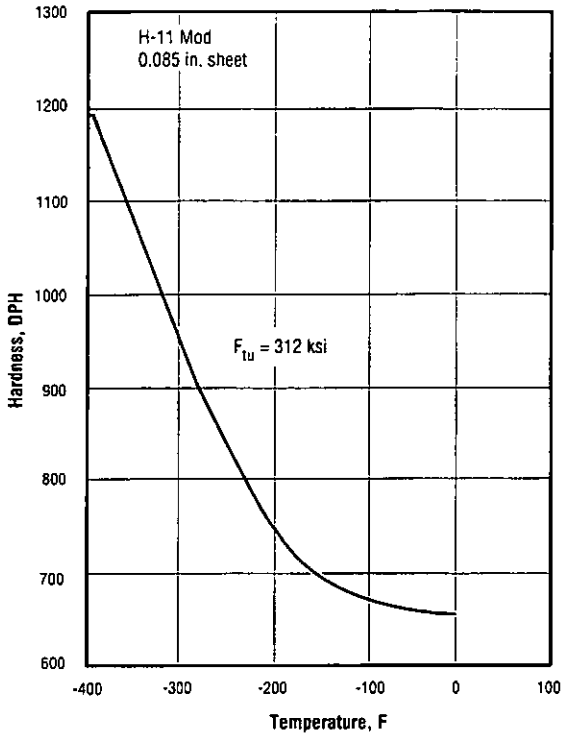

Fig. 1.6.7 Effect of low temperature on hardness of sheet (Ref. 26)

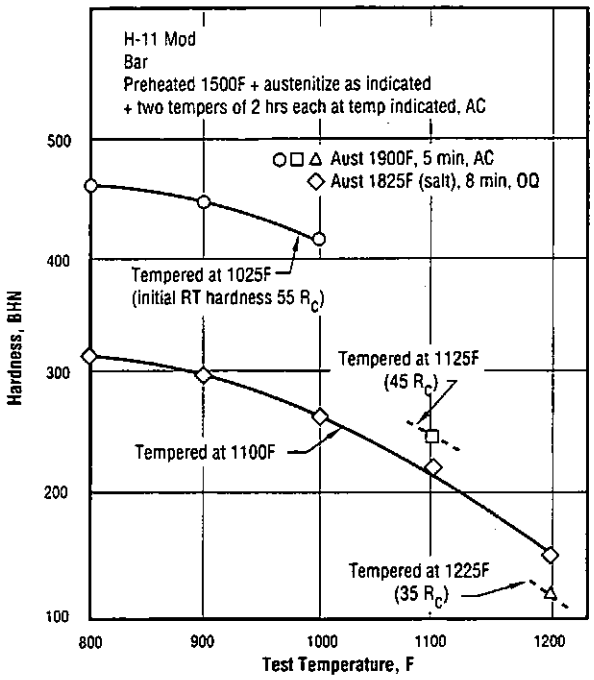

Fig. 1.6.8 Hot hardness of bar austenitized at 1825 or 1900F, and tempered at temperatures from 1025 to 1225F (Ref. 38)

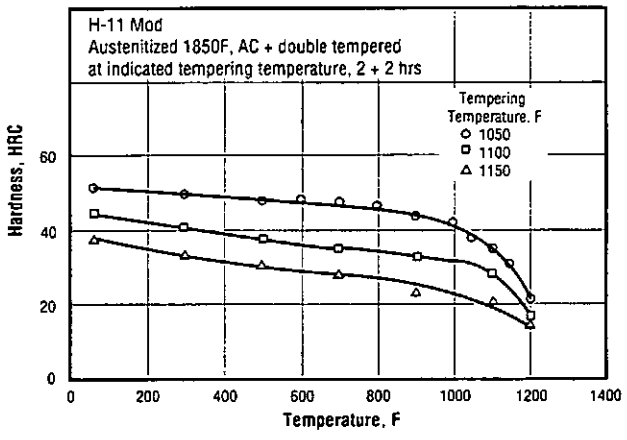

Fig. 1.6.9 Hot hardness after tempering at 1050 to 1150F (Ref. 81)

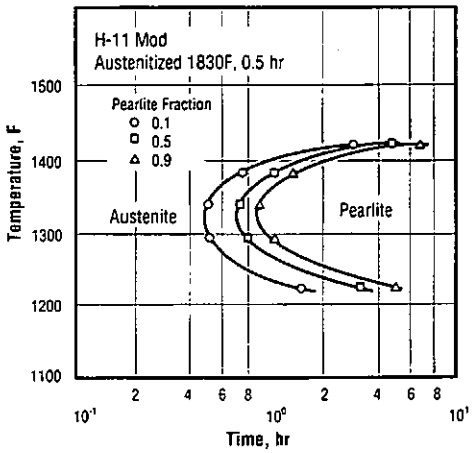

Fig. 2.1.2.1 Time-temperature-transformation diagram (Ref. 87)

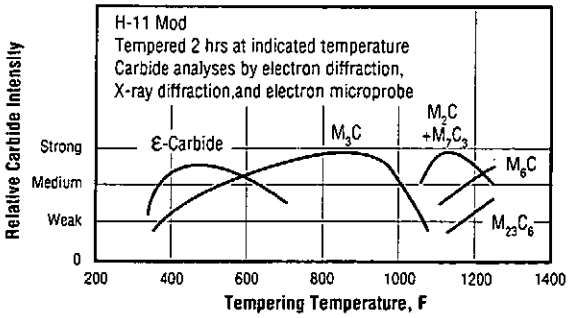

Fig. 2.1.2.4 Relative carbide intensity (abundance) as a function of tempering temperature (Ref. 88)

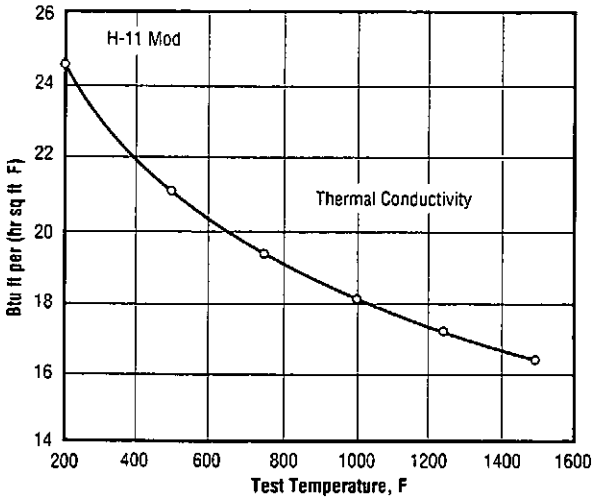

Fig. 2.1.3.1 Thermal Conductivity (Ref. 38)

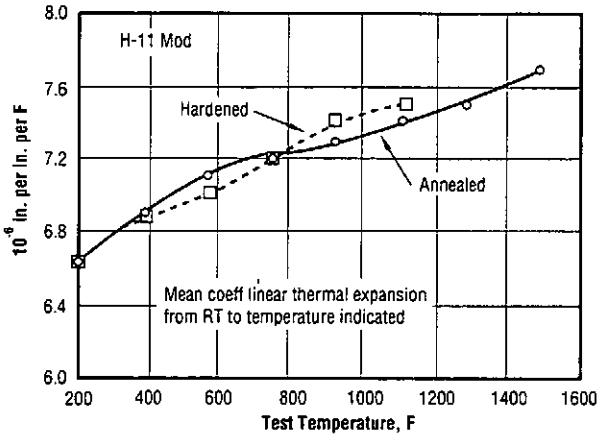

Fig. 2.1.4.1 Thermal Expansion (Ref. 38)

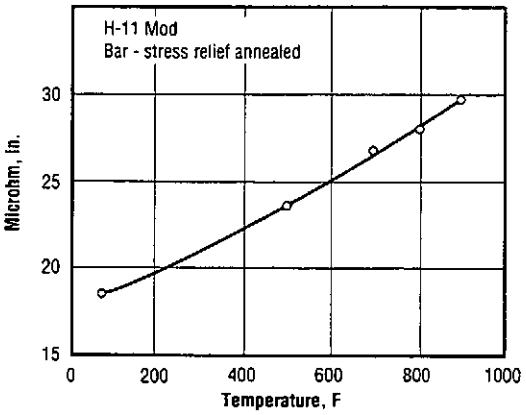

Fig. 2.2.2.1 Electrical Resistivity (Ref. 75)

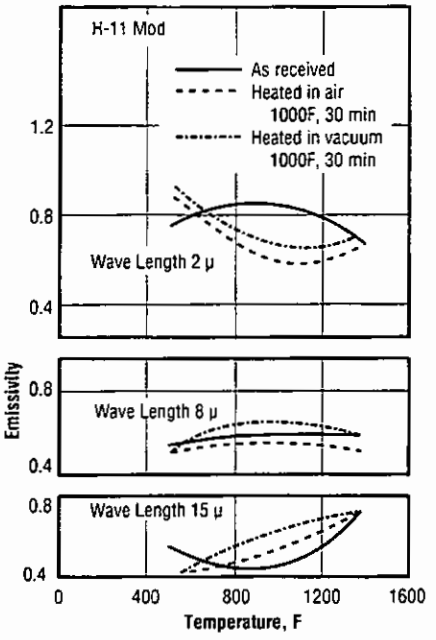

Fig. 2.2.4.1 Emittance (Ref. 25)

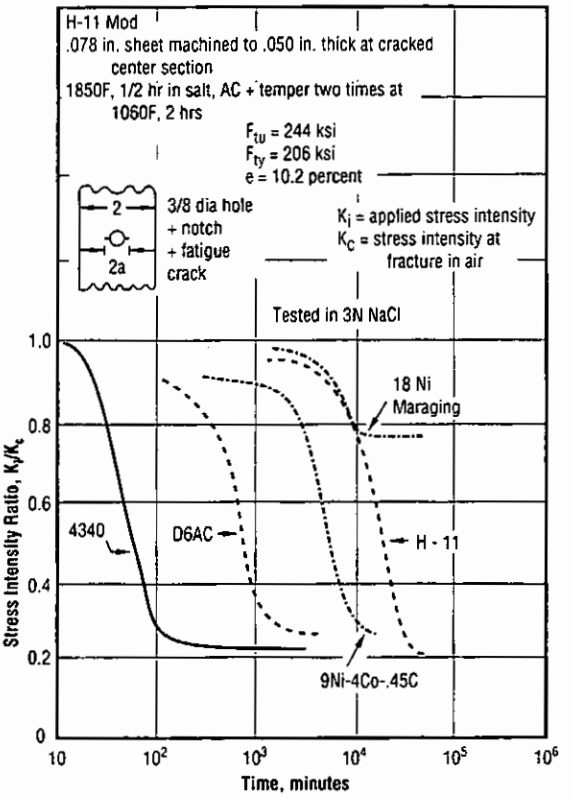

Fig. 2.3.2.2 Comparison of stress corrosion cracking characteristics of alloy with corresponding behavior of several other martenistic steels heat treated to tensile strength levels of approximately 240 ksi (Ref. 56)

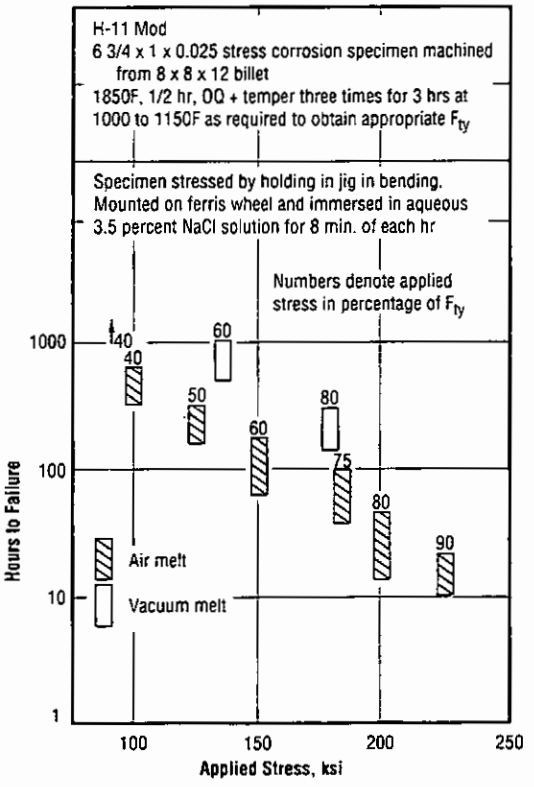

Fig. 2.3.2.3 Effect of applied stress on time to stress corrosion failure for air melt and vacuum melt alloy (Ref. 63)

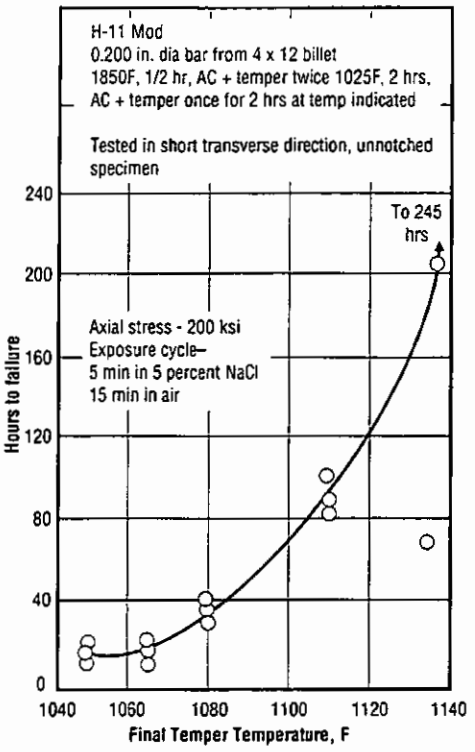

Fig. 2.3.2.4 Effect of temperature of final temper on stress-corrosion resistance in 5 percent aqueous solution of NaCl (Ref. 62)

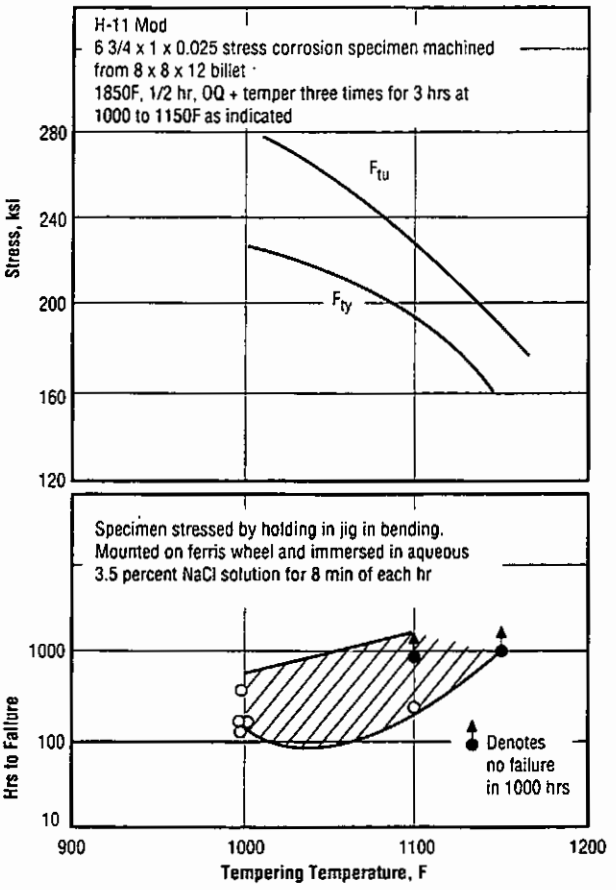

Fig. 2.3.2.5 Effect of tempering temperature on stress-corrosion resistance of billet (Ref. 63)

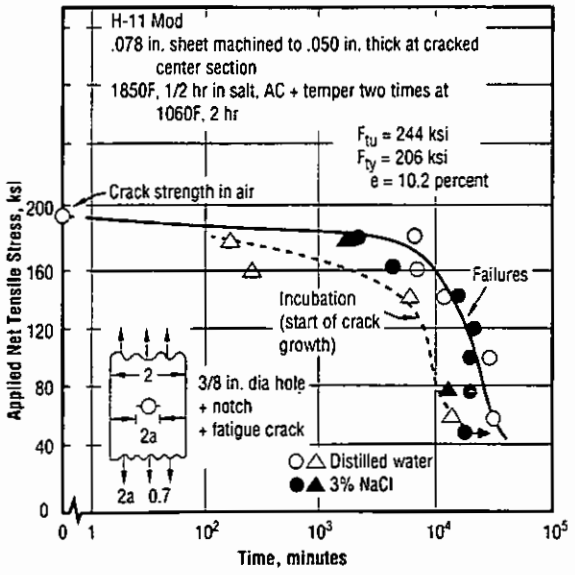

Fig. 2.3.2.6 Delayed failure of alloy at 206 ksi yield strength level when tested in distilled water and in aqueous solution containing 3 percent NaCl (Ref. 56)

Table 2.3.2.7 Plane strain fracture toughness and threshold for stress corrosion cracking in seacoast test and in accelerated tests for alloy in three conditions (Ref. 47)

Alloy: H-11 Mod			
Form	**1/4 in. sheet (a)**		
Condition	**Vac. Melt 2+2 hr @ 1000F F_{ty} 280-300 ksi**	**Air Melt 2+2 hr @ 1000F F_{ty} 280-300 ksi**	**Air Melt 2+2 hr @ 1100F F_{ty} 220-240 ksi**
K_{Ic} (ksi $\sqrt{in}$)	28.5	27.6	52.8
K_{Iscc} (ksi $\sqrt{in}$)			
Seacoast (b)	11.4 ± 5.6	16.7 ± 2.8	39.5 ± 4.4
Accelerated (c)	10.8 ± 1.9	8.6 ± 1.4	23.2 ± 0.2

(a)

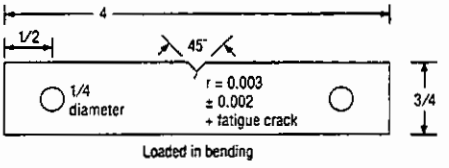

(b) One face exposed to Pacific Ocean (L.A. Dept. of Water & Power)
(c) Immersed in solution of 200g NaCl per liter distilled water.

Table 2.3.2.8 Plane strain fracture toughness and threshold for stress corrosion cracking in 3-1/2 percent NaCl aqueous solution (Ref. 52)

Alloy: H-11 Mod			
Form	**1/2 plate**		
Condition	**Quenched and tempered at 1100F**		
	F_{ty} (ksi)	**K_{Ic} (ksi $\sqrt{in}$)**	**K_{Iscc} (ksi $\sqrt{in}$)**
	188	54	30

Tested at RT in water containing 3-1/2 percent NaCl.

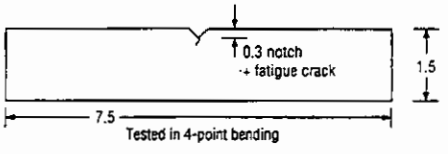

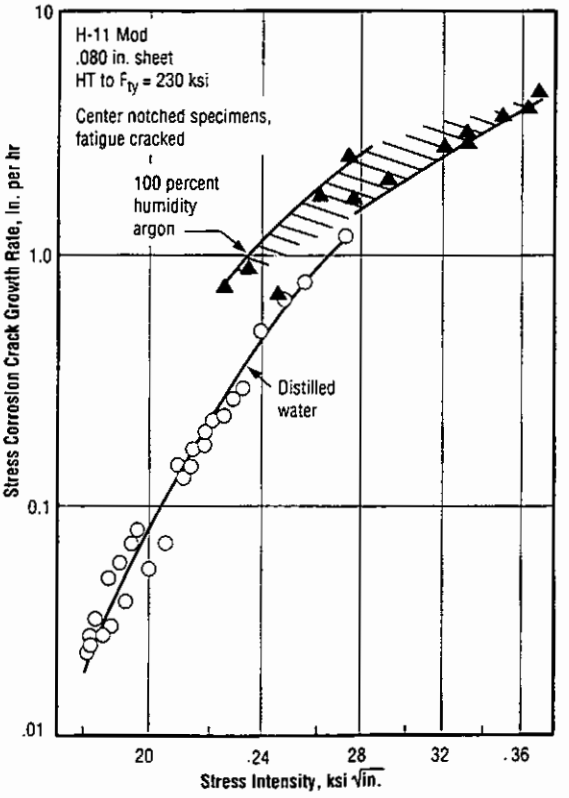

Fig. 2.3.2.9 Sustained load crack growth rate in humid argon and in distilled water (Ref. 53)

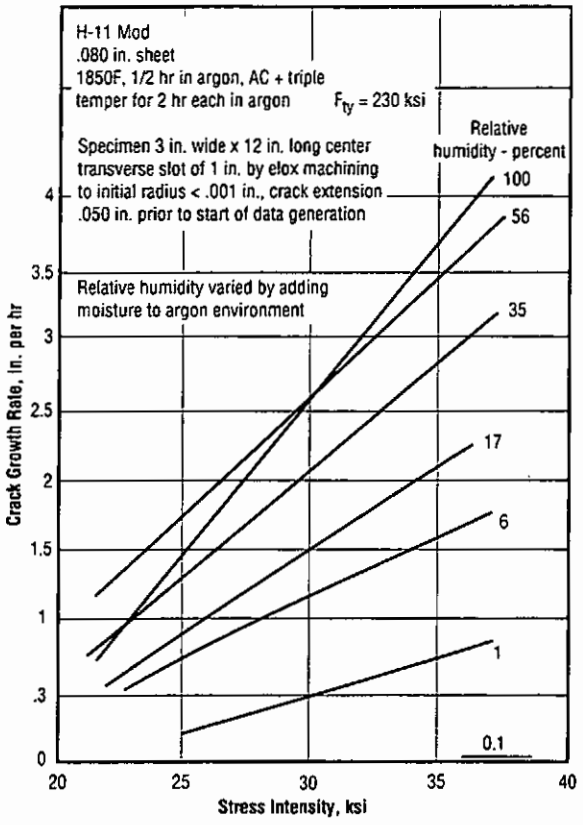

Fig. 2.3.2.10 Effect of stress intensity on crack growth rate for a wide range of relative humidity in an argon environment (Ref. 41)

Table 2.3.3.3 Notch strength in helium and hydrogen at 10 ksi pressure (Ref. 46)

Alloy: H-11 Mod		
Form (a)	1 in bar machined to notch shown 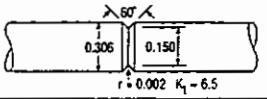	
Condition	**1850F, 40 min. AC + triple temper 1000F, 2 hr AC**	
	Notch strength (a) (ksi)	**Ductility (RA)**
Helium	253	0
Hydrogen	62	0
Hydrogen after 1 hr hold at 50 ksi	65	0
Hydrogen after 100 hr hold at 50 ksi	103	0

(a) Average of replicate tests with small variations in geometry and strength values.

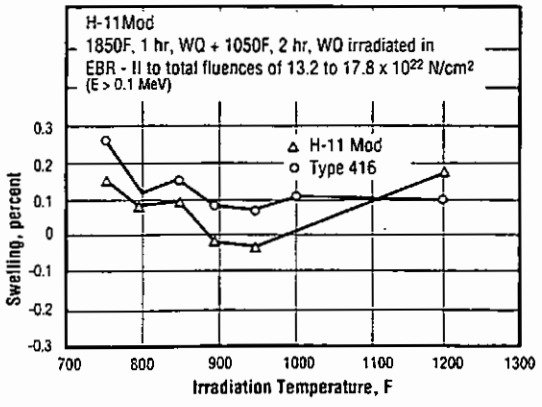

Fig. 2.4.2 Effect of irradiation temperature on swelling in H-11 Mod and Type 416 martensitic stainless steel (Ref. 92)

Table 3.1.1 AMS-Specified Mechanical Properties (Refs. 77-80)

Alloy: H-11 Mod						
AMS Specification	**6437D**	**6485F**			**6487F, 6488D**	
Form	**Sheet, Strip, and Plate**	**Bars & Forgings**			**Bars & Forgings (premium quality)**	
Heat Treatment	**Austenitize 1825-1875F, 15-25 min, AC**	**Austenitize 1825-1875F, 15-45 min, AC**				
	Triple Temper, 1000F, 2-3 Hr					
Test Temperature	**RT**	**RT**		**1000F**	**RT**	
Test Orientation	**L**	**L**	**T**	**L**	**L**	**T (c)**
Tensile Properties						
F_{tu} (ksi, min)	260	260	260	175	260	260 (d)
F_{ty} (ksi, min)	220	215	215	135	215	215
e (pct, min) (a)	5	8		10	8	6
RA (pct, min)		30		35	30	
Cross-section area (square inch)						
25 to 75			6			
75 to 100			6			
100 to 150			5			
150 to 225			4			
225 to 256						
Bend Properties						
Angle (deg, min) (b) Thickness (inch)						
up to .250	180					
.250 to .437	90					

Note: The original AMS documents should be consulted for complete specification details.
(a) 2 inches or 4 D
(b) Free bend around 3 T diameter
(c) 6488D only
(d) 280 ksi max

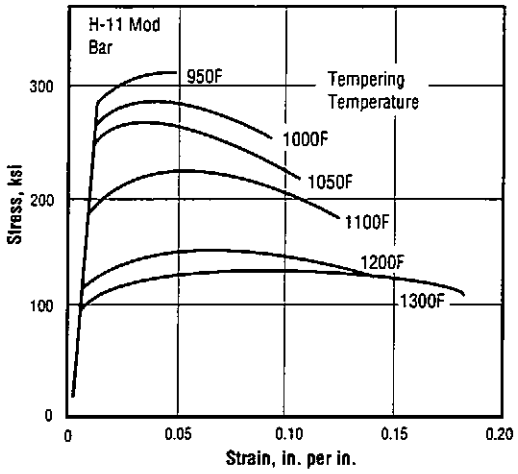

Fig. 3.2.1.1.1 Stress strain curves for bar tempered at 950 to 1300F (Ref. 9)

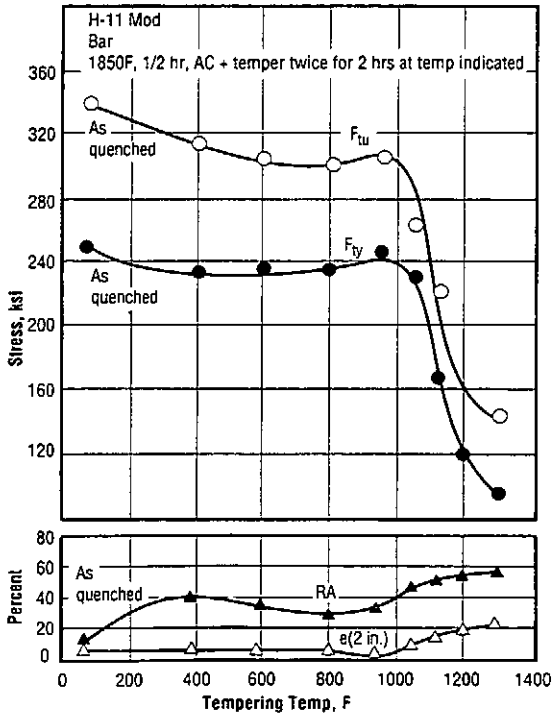

Fig. 3.2.1.2.2 Effects of tempering up to 1300F on tensile properties of bar (Ref. 40)

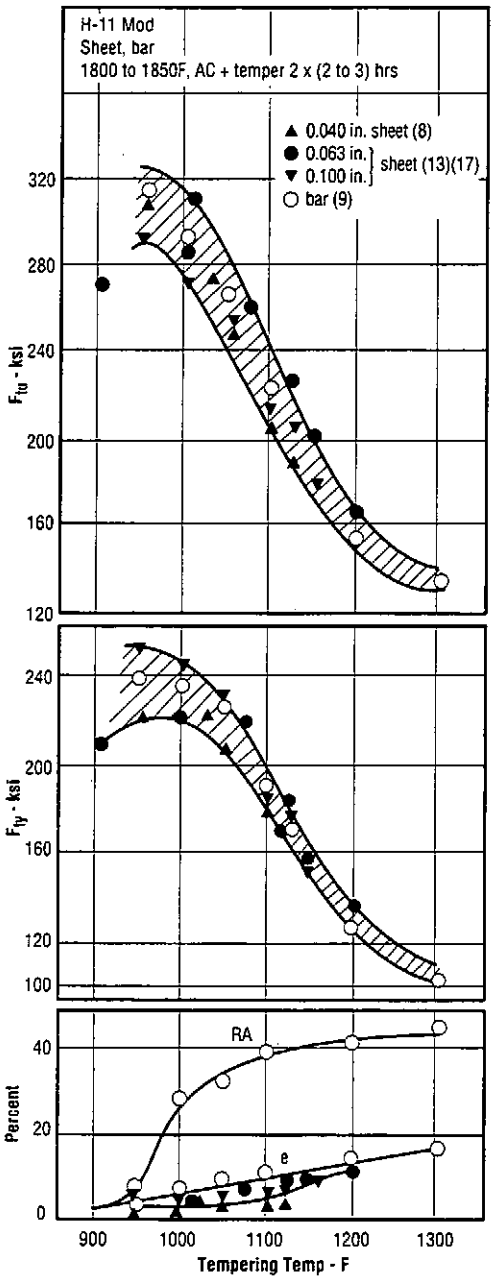

Fig. 3.2.1.2.1 Effect of tempering at 900 to 1300F on tensile properties of sheet and bar (Ref. 8, 9, 13, 17)

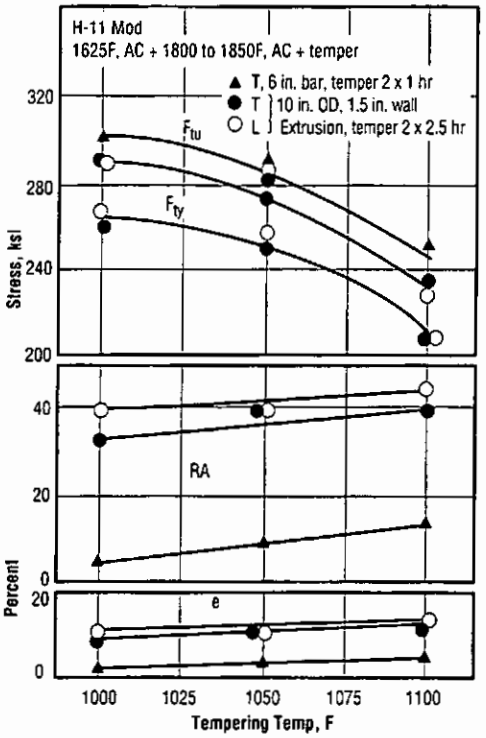

Fig. 3.2.1.2.3 Effects of tempering at 1000 to 1100F on transverse tensile properties of bar and extrusions (Ref. 16)

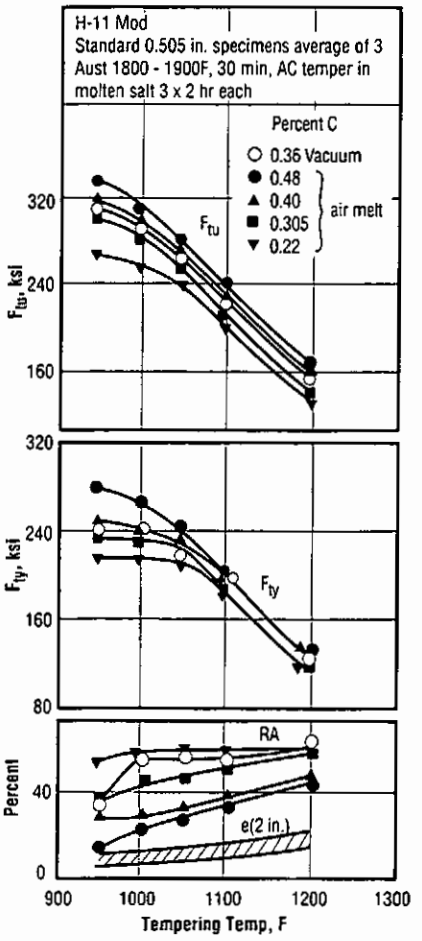

Fig. 3.2.1.2.4 Effects of carbon content and tempering temperature on tensile properties of air melted and vacuum melted alloy. (Ref. 22)

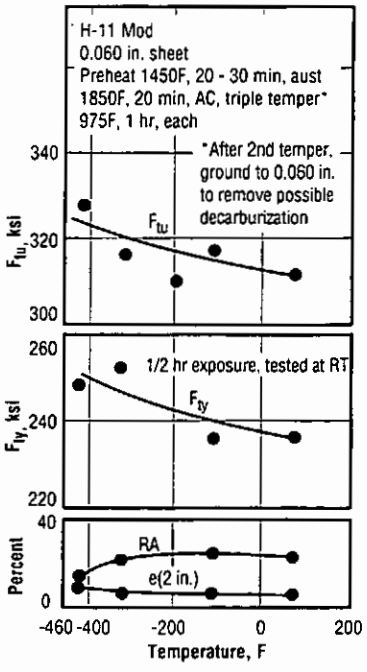

Fig. 3.2.1.3.1 Effects of low temperature exposure on tensile properties of sheet (Ref. 26)

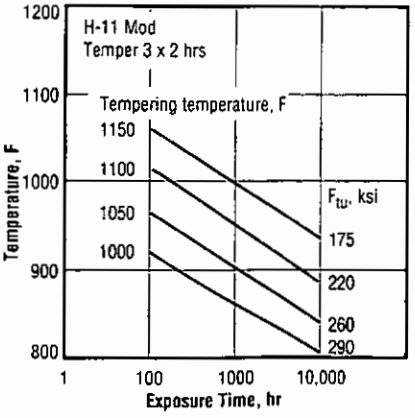

Fig. 3.2.1.3.2 Maximum temperatures for stability of mechanical properties for various exposure times (Ref. 6)

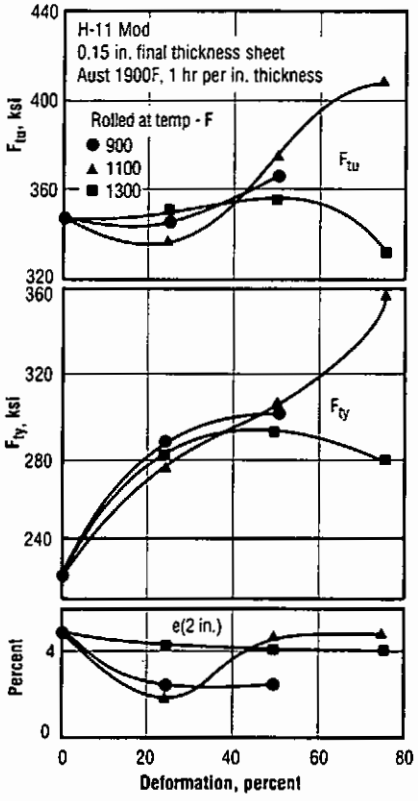

Fig. 3.2.1.4.1 Effects of rolling on tensile properties of austenitized sheet (Ref. 31)

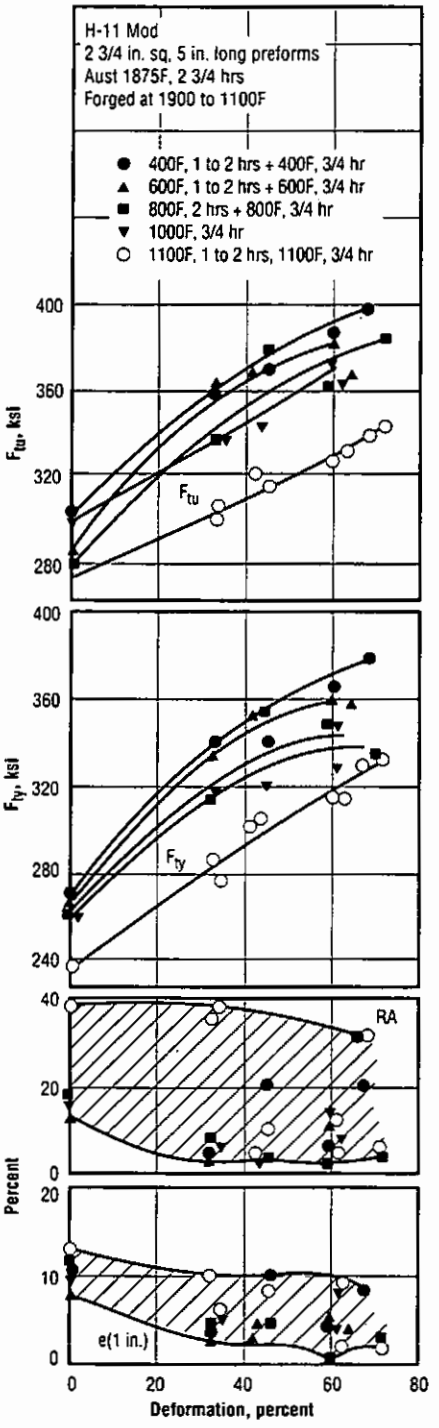

Fig. 3.2.1.4.2 Effects of forging and tempering on tensile properties of austenitized steel (Ref. 32)

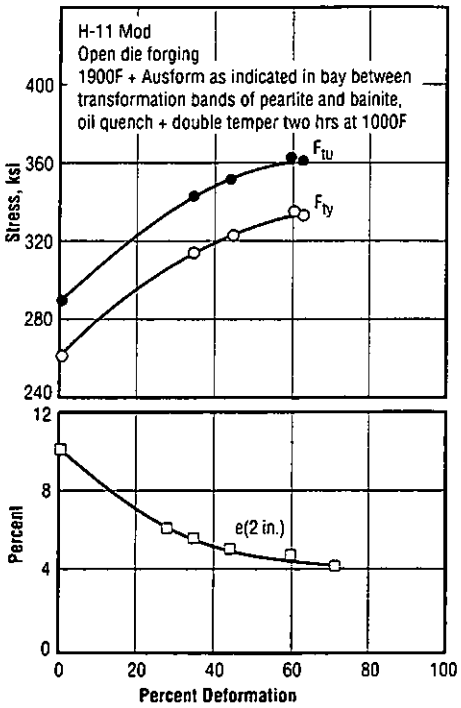

Fig. 3.2.1.4.3 Effects of forging and tempering on tensile properties of vacuum melted alloy (Ref. 69)

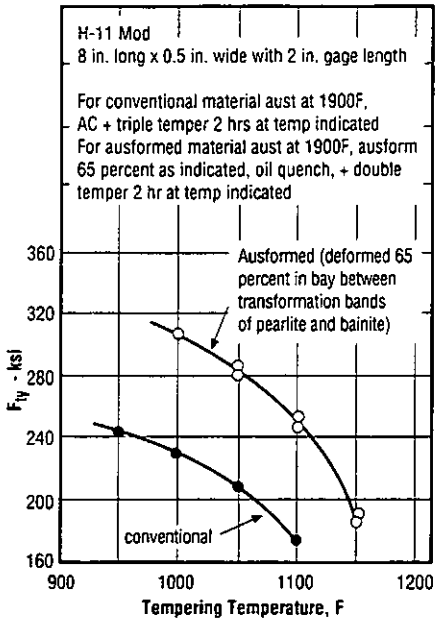

Fig. 3.2.1.4.4 Effects of tempering temperature on yield strength for conventional alloy and for ausformed alloy (Ref. 69)

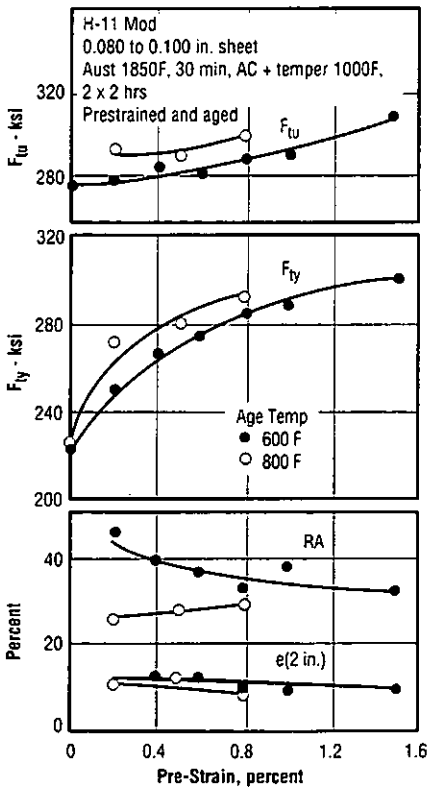

Fig. 3.2.1.4.5 Effects of pre-straining on tensile properties of austentized and tempered sheet (Ref. 36)

Table 3.2.1.5.1 Tensile properties of bar in air at atmospheric pressure and in helium and hydrogen at 10 ksi pressure (Ref. 46)

Alloy: H-11 Mod			
Form	**1 inch bar machined to tensile spec.**		
Condition	**1850F, 40 min., AC + triple temper 1000F, 2 hr, AC**		
	F_{tu} (ksi)	**e, 1 in. (pct)**	**RA (pct)**
Air at atmosphere press	293	11	30
He at 10 ksi press	299	8.8	30
He (hydrogen contaminated) at 10 ksi press	278	1.4	1.2
Hydrogen, at 10 ksi press	170	0	0
Hydrogen, after 1 hr hold at 128 ksi stress	171	0	0
Hydrogen, after 100 hr hold at 128 ksi stress	166	0	0

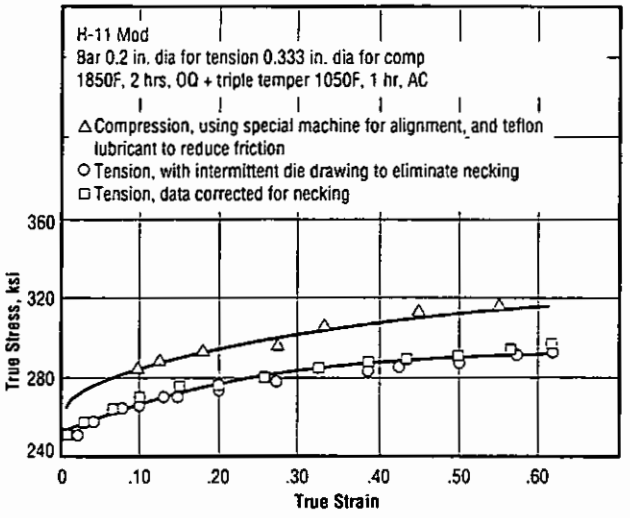

Fig. 3.2.2.1 True stress - true strain curves in tension and compression of bar (Ref. 43)

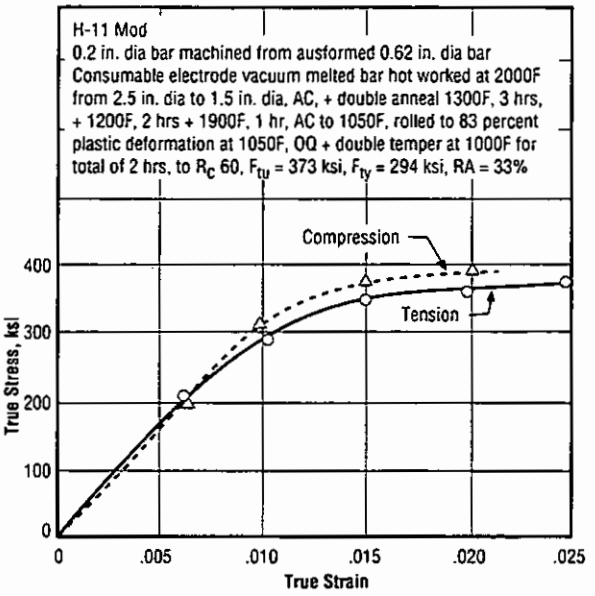

Fig. 3.2.2.2 True stress - true strain curves in tension and compression for ausformed bar (Ref. 64)

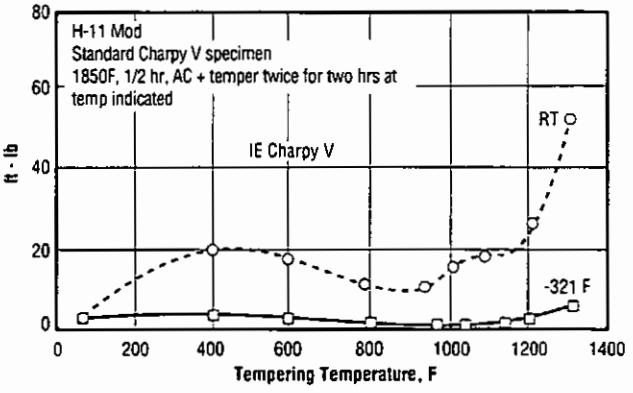

Fig. 3.2.3.2 Effect of tempering temperature on Charpy impact energy at RT and -321F (Ref. 40)

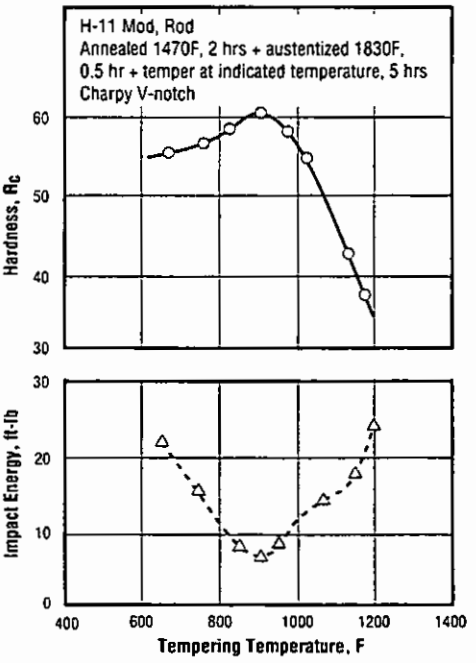

Fig. 3.2.3.3 Effects of tempering temperature on Charpy impact energy and hardness (Ref. 93,)

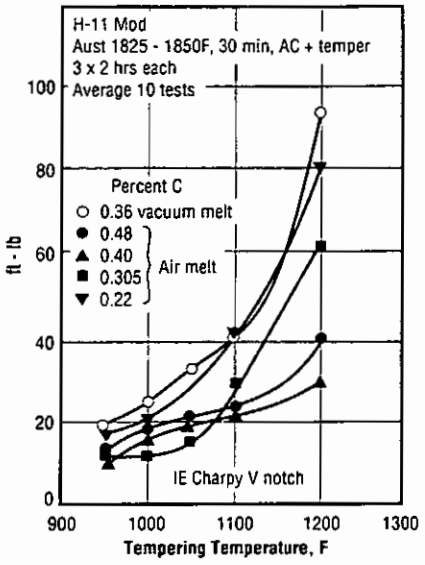

Fig. 3.2.3.4 Effect of carbon content and tempering temperature on Charpy impact strength of air melt and vacuum melt alloy (Ref. 22)

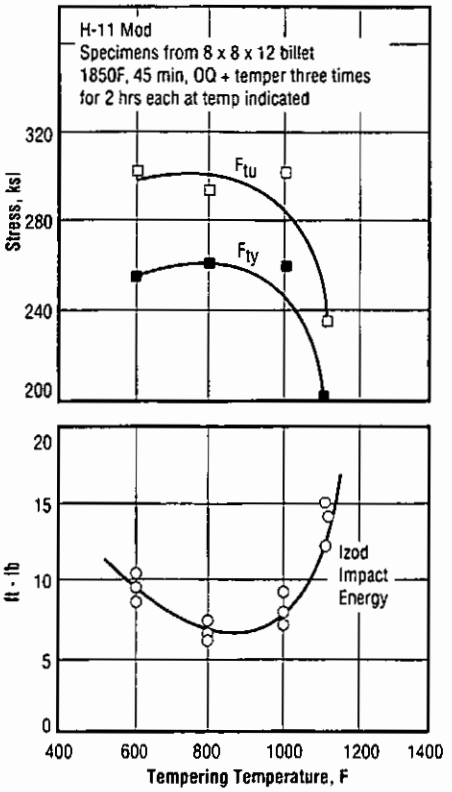

Fig. 3.2.3.5 Effect of tempering temperature on tensile and yield strength and on Izod impact energy (Ref. 63)

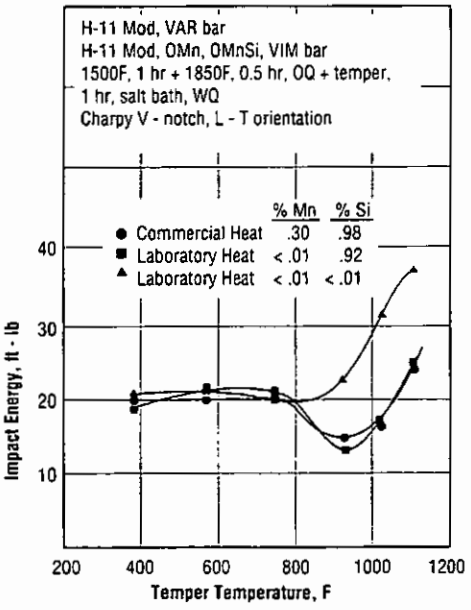

Fig. 3.2.3.7 Effects of tempering temperature and manganese and silicon contents on Charpy impact energy (Ref. 94)

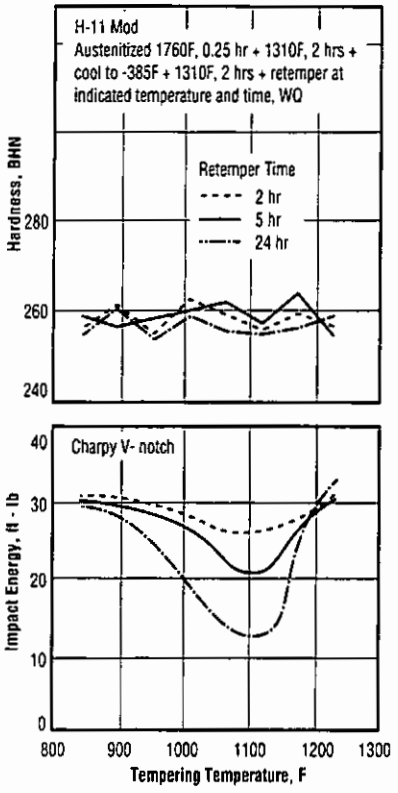

Fig. 3.2.3.8 Effects of retempering time and temperature on Charpy impact energy and hardness (Ref. 93)

Table 3.2.6.1 Typical bearing and shear properties (Ref. 4)

Alloy: H-11 Mod						
Form	**Sheet**					
Condition F_{tu} (ksi)	**260 to 280**			**280 to 300**		
Thickness (in.)	**0.063**	**0.063**	**0.078**	**0.063**	**0.063**	**0.078**
F_{bru} (ksi)						
e/D=1.5 L	-	-	378	-	-	432
e/D=2.0 L	512	477	-	547	525	-
e/D=2.0 T	509	-	-	529	-	-
F_{bry} (ksi)						
e/D=1.5 L	-	-	316	-	-	369
e/D=2.0 L	364	338	-	388	380	-
e/D=2.0 T	371	-	-	392	-	-
F_{su} (ksi) L	170	166.5	170	178	184	186
F_{su} (ksi) T	171	169	171	183	186	187.5
F_{su}/F_{tu} (avg)	0.631	0.635	0.642	0.634	0.635	0.635

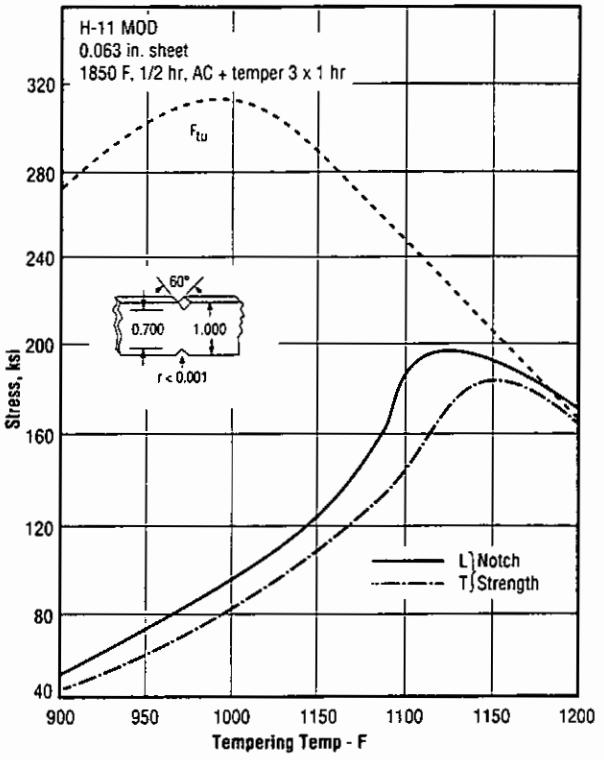

Fig. 3.2.7.1.2 Effects of tempering temperature on notch strength of sharply notched sheet. (Ref. 13)

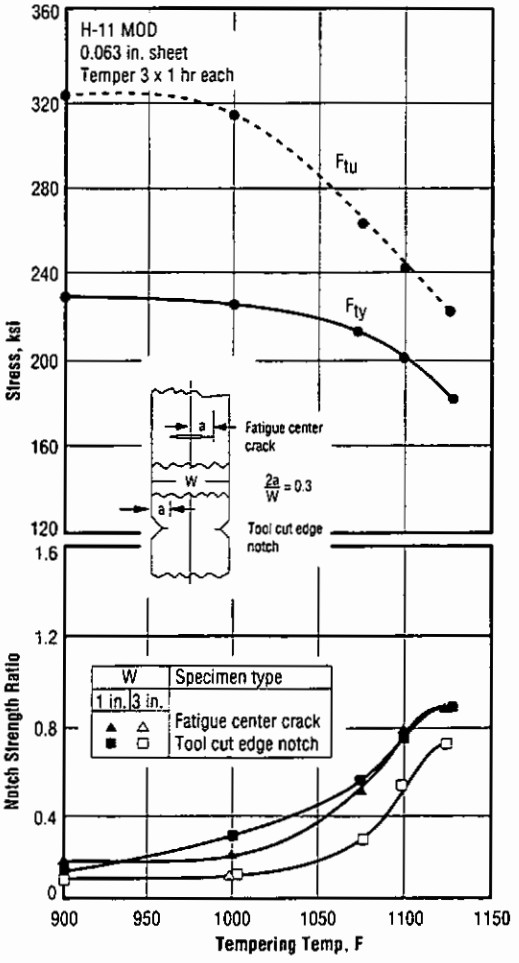

Fig. 3.2.7.1.3 Effects of tempering temperature on sharp notch strength ratio for sheet. (Ref. 27)

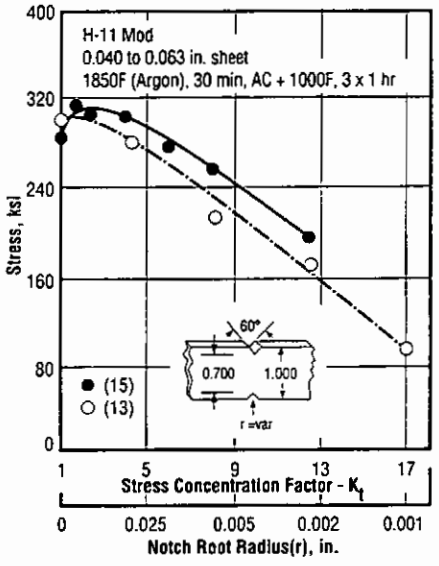

Fig. 3.2.7.1.4 Effects of stress concentration on notch strength of heat treated sheet. (Refs. 13, 15)

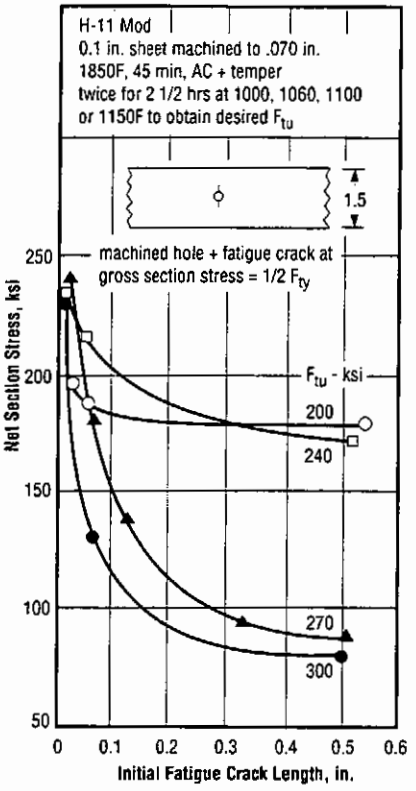

Fig. 3.2.7.1.5 Effects of initial crack length on net section strength for sheet heat treated to F_{tu} from 200 to 300 ksi (Ref. 58)

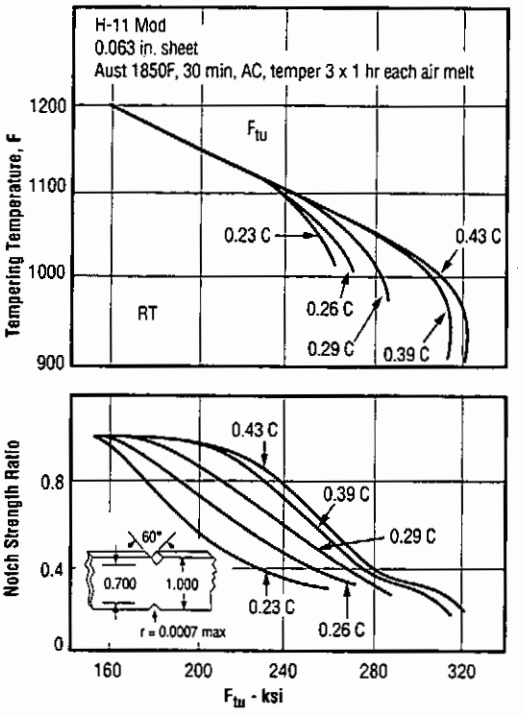

Fig. 3.2.7.1.6 Effect of carbon content and strength on sharp edge notch tensile strength ratio of air melt and vacuum melt sheet (Ref. 17)

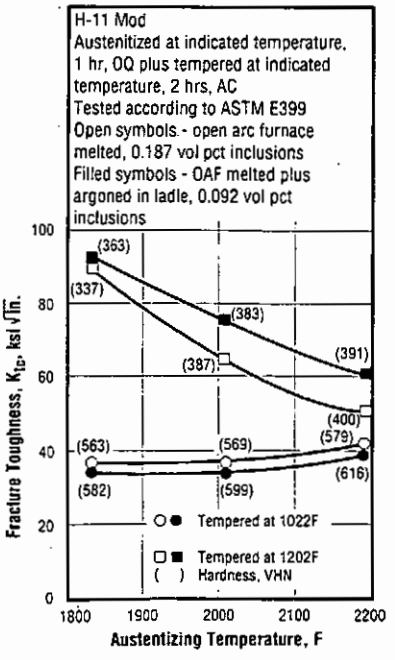

Fig. 3.2.7.2.2 Effects of austenitizing temperature, tempering temperature, and melting practice on fracture toughness (Ref. 95)

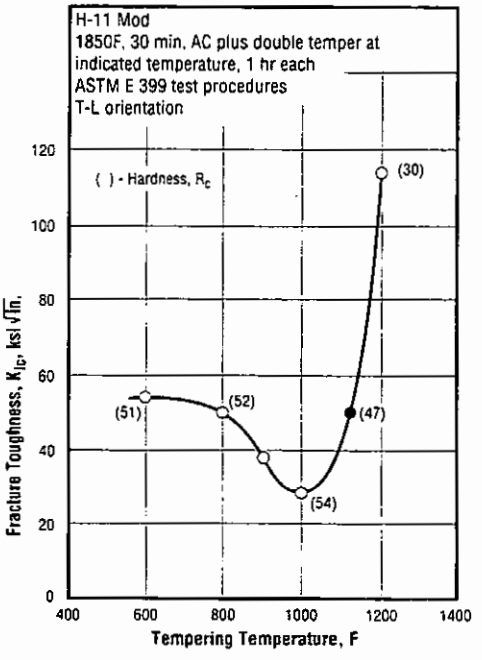

Fig. 3.2.7.2.3 Effect of tempering temperature on fracture toughness (Ref. 96)

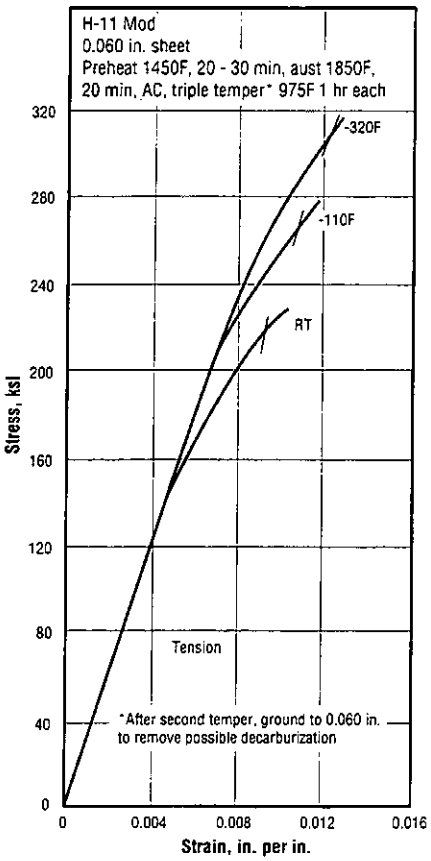

Fig. 3.3.1.1 Stress-strain curves at room and low temperatures for sheet (Ref. 26)

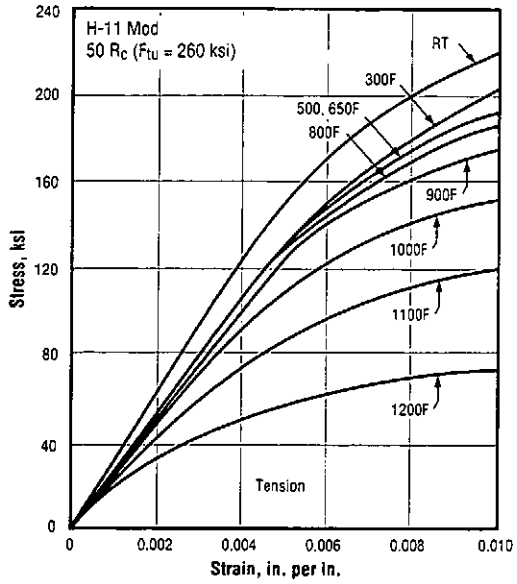

Fig. 3.3.1.2 Stress-strain curves at room and elevated temperatures for material heat treated to F_{tu} = 260 ksi (Ref. 9)

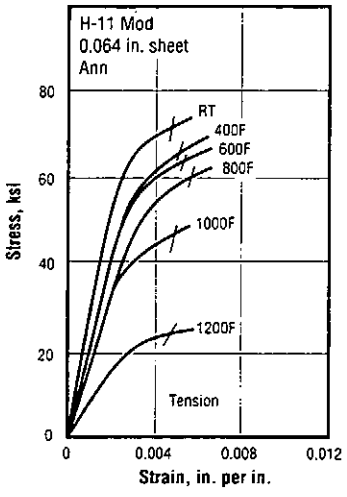

Fig. 3.3.1.3 Stress - strain curves at room and elevated temperatures for annealed sheet (Ref. 34)

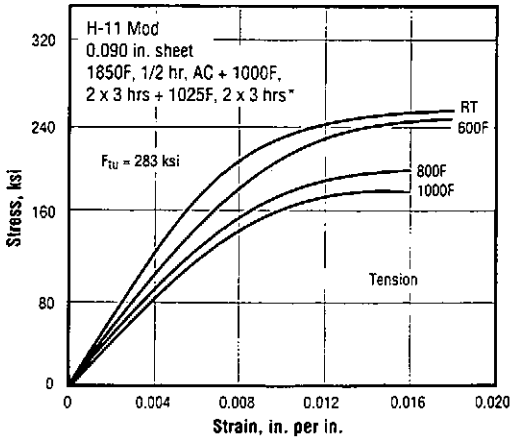

Fig. 3.3.1.4 Stress-strain curves at room and elevated temperatures for sheet heat treated to F_{tu} = 280 ksi (Ref. 7)

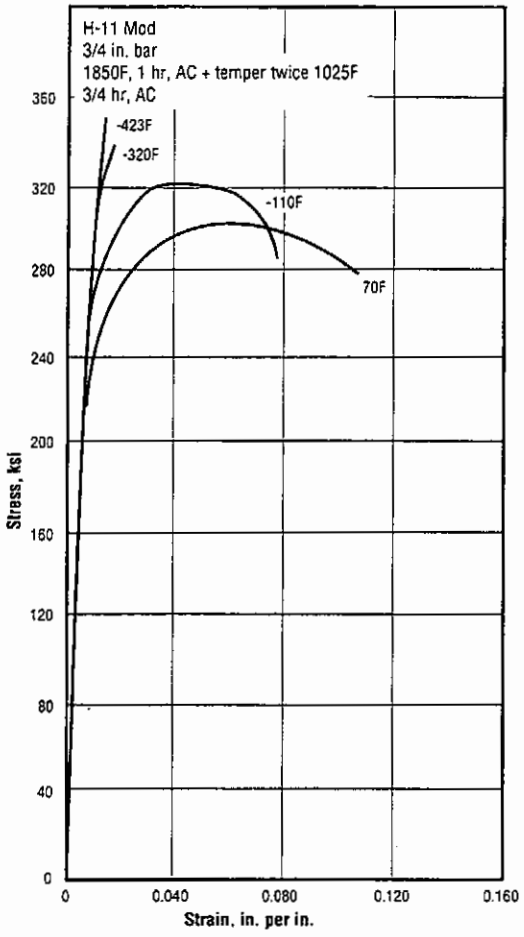

Fig. 3.3.1.5 Stress-strain curves at room and low temperatures for bar (Ref. 67)

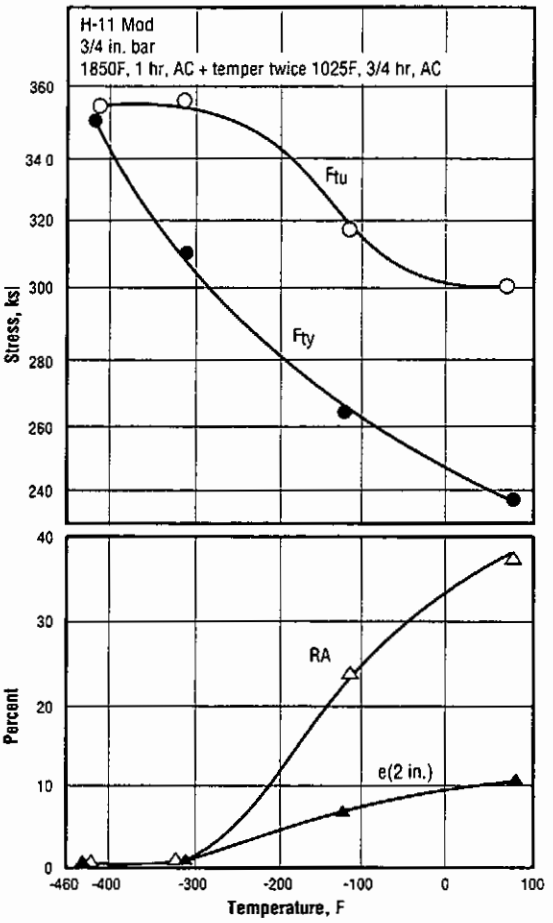

Fig. 3.3.1.6 Effect of low test temperature on tensile properties of bar. (Ref. 67)

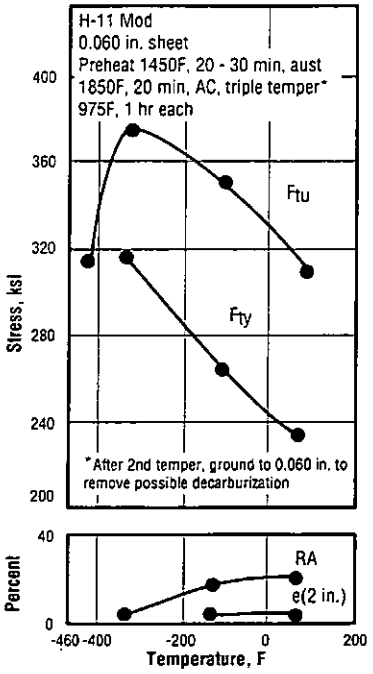

Fig. 3.3.1.7 Effect of low test temperature on tensile properties of sheet (Ref. 26)

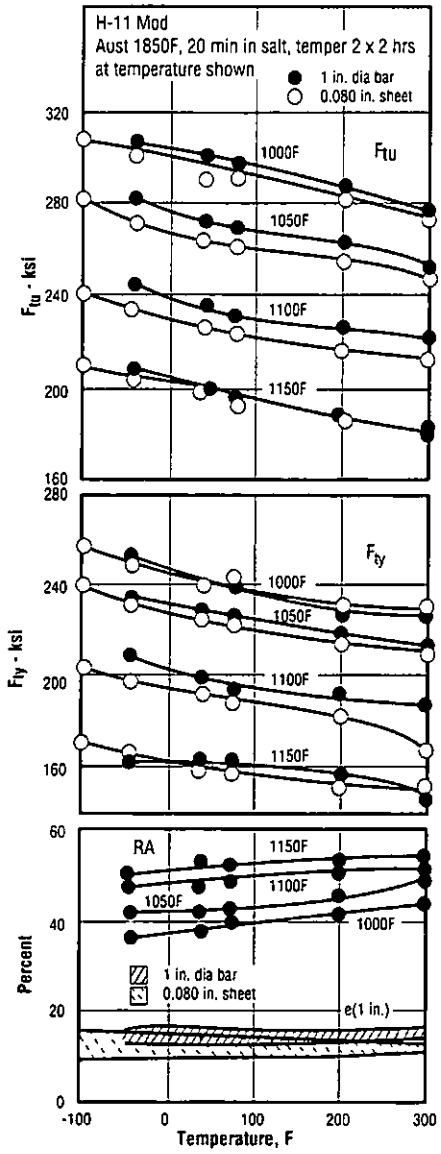

Fig. 3.3.1.8 Effect of test temperature on tensile properties for tempering temperatures of 1000 to 1150F of bar and sheet (Ref. 30)

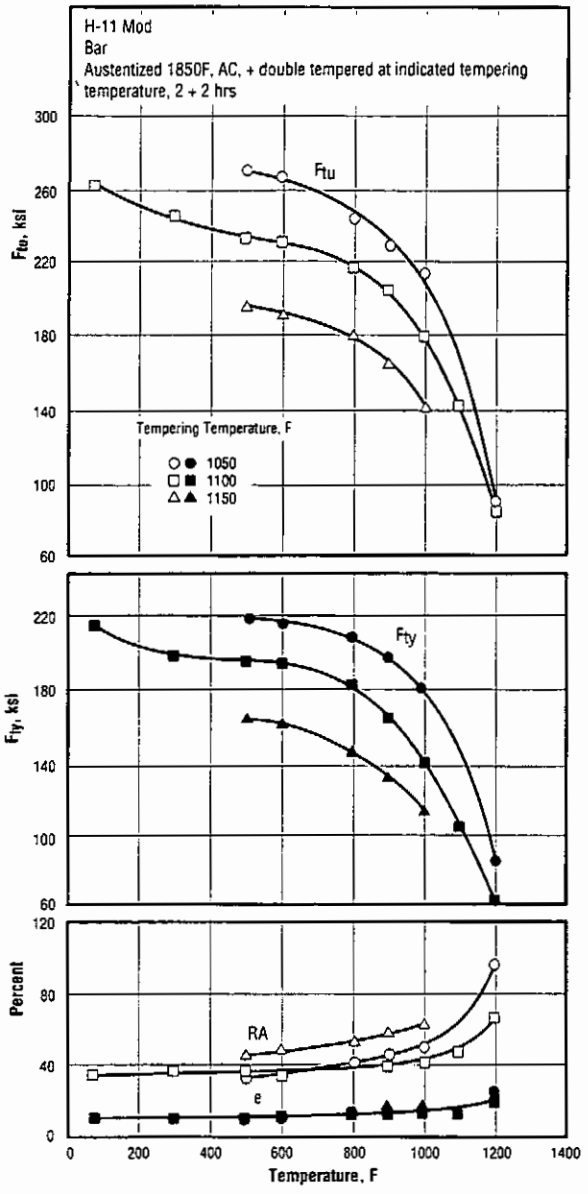

Fig. 3.3.1.9 Effects of test temperature and tempering temperature on tensile properties of bar (Ref. 81)

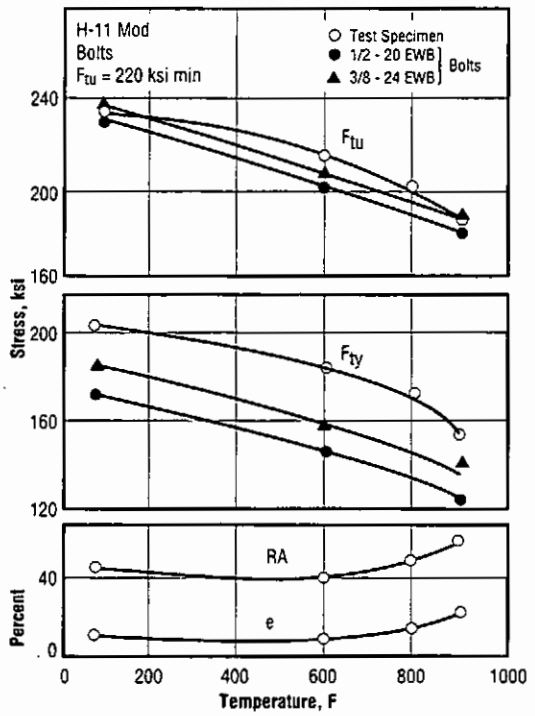

Fig. 3.3.1.10 Effect of test temperature on tensile properties of bolts heat treated to F_{tu} = 220 ksi minimum (Ref. 10)

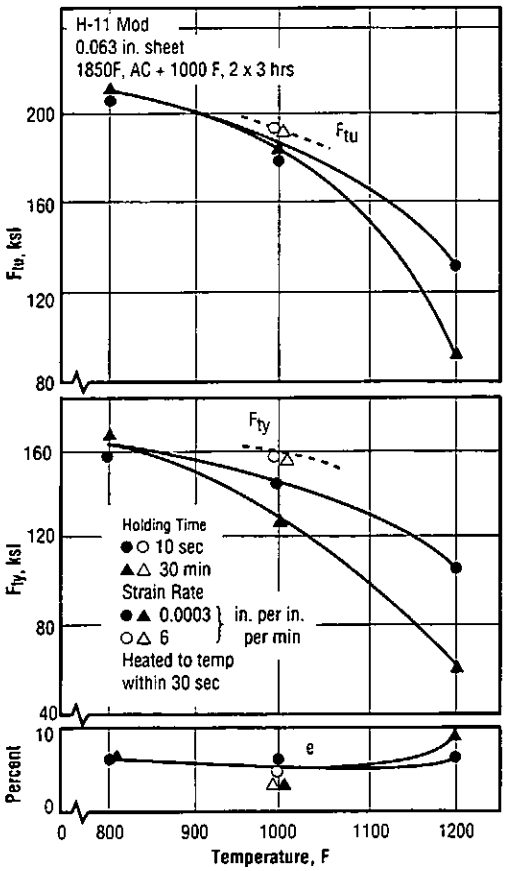

Fig. 3.3.1.11 Effects of test temperature, holding time and strain rate on tensile properties of sheet (Ref. 20)

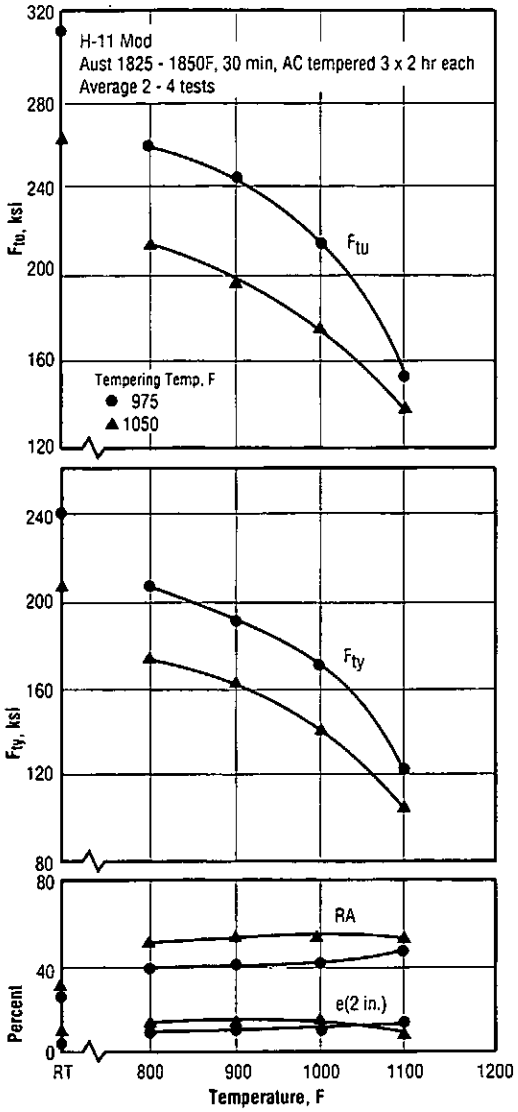

Fig. 3.3.1.12 Effect of test temperature on tensile properties of air melt alloy tempered to F_{tu} = 260 ksi and 310 ksi (Ref. 22)

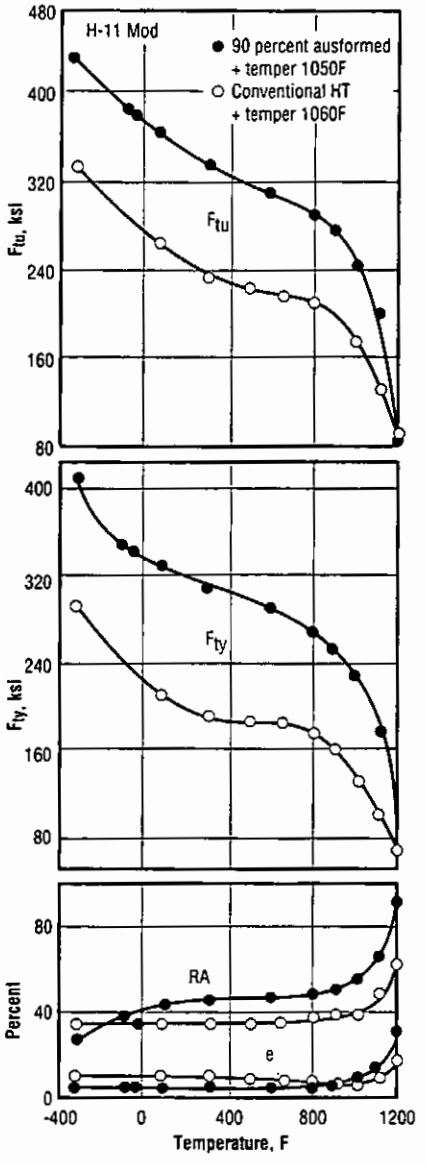

Fig. 3.3.1.13 Effect of test temperature on tensile properties of ausformed and conventionally heat treated steel (Ref. 37)

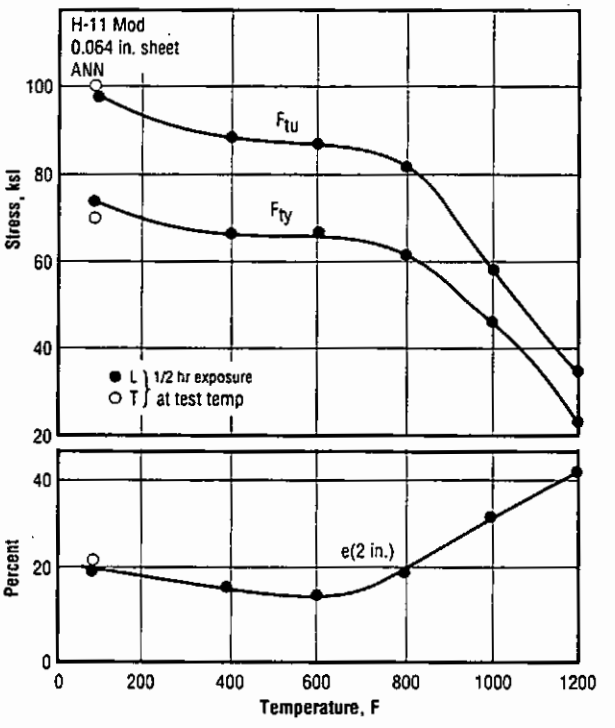

Fig. 3.3.1.14 Effect of test temperature on tensile properties of annealed sheet (Ref. 34)

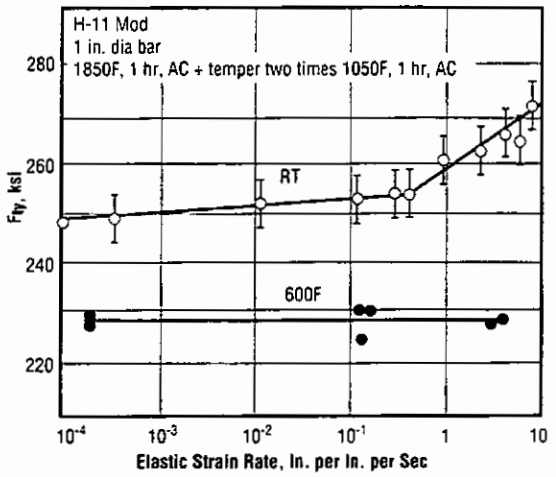

Fig. 3.3.1.15 Effect of elastic strain rate on yield stress at RT and 600F (Refs. 65, 66)

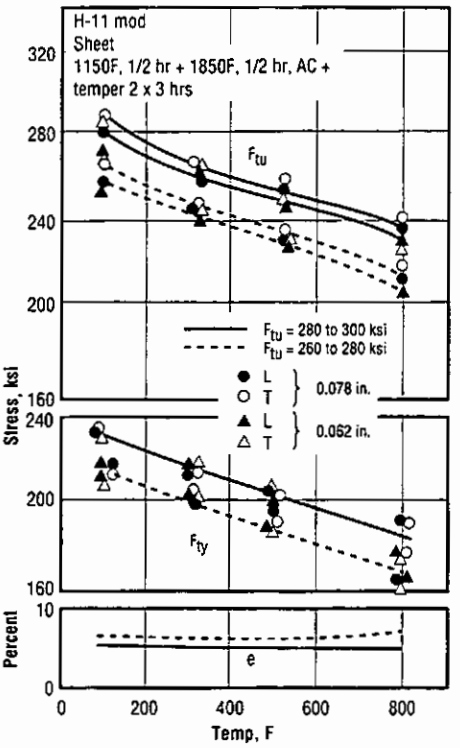

Fig. 3.3.1.16 Effect of test temperature on tensile properties of sheet heat treated to F_{tu} = 260 and 280 ksi minimum (Refs. 4, 5)

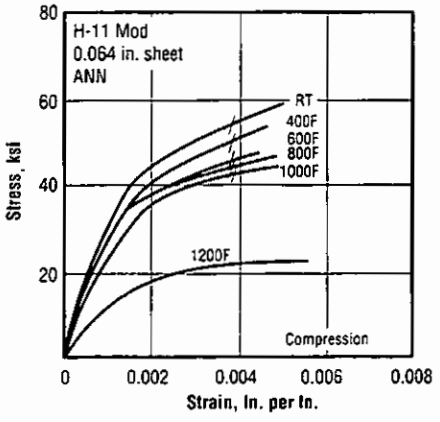

Fig. 3.3.2.1 Stress-strain curves in compression at room and elevated temperatures for annealed sheet (Ref. 34)

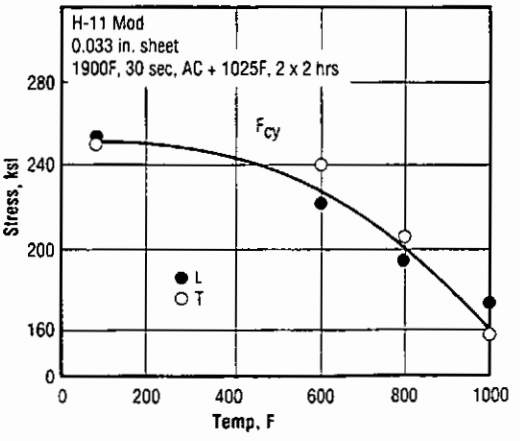

Fig. 3.3.2.2 Effect of test temperature on compressive yield strength of sheet (Ref. 7)

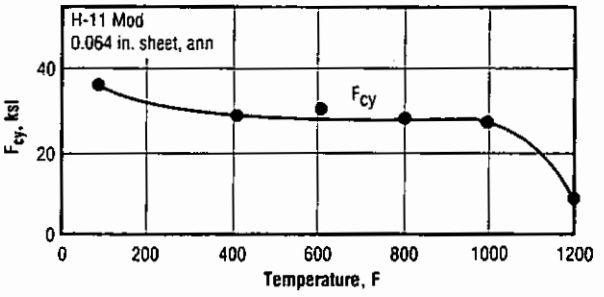

Fig. 3.3.2.3 Effect of test temperature on compressive yield strength of annealed sheet (Ref. 34)

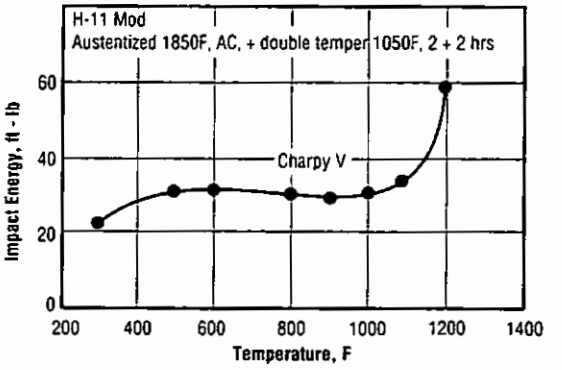

Fig. 3.3.3.1 Effect of temperature on Charpy impact energy of bar (Ref. 81)

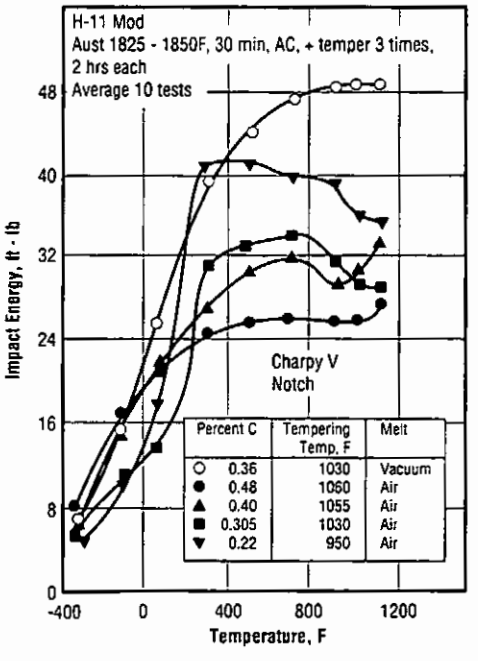

Fig. 3.3.3.2 Effect of carbon content and test temperature on Charpy impact strength of air melt and vacuum melt alloy (Ref. 22)

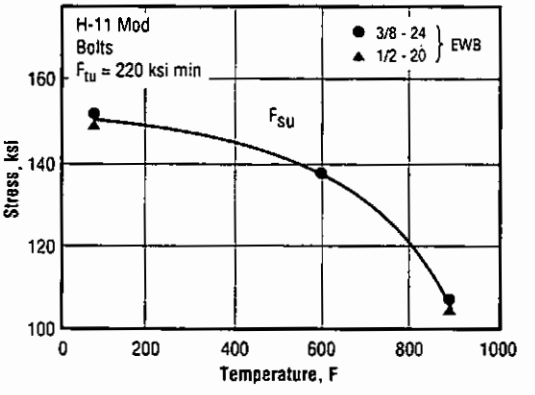

Fig. 3.3.5.1 Effect of test temperature on shear strength of heat treated bolts (Ref. 10)

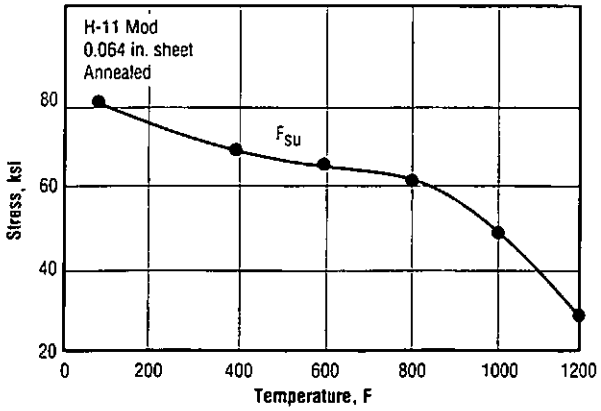

Fig. 3.3.5.2 Effect of test temperature on shear strength of annealed sheet (Ref. 34)

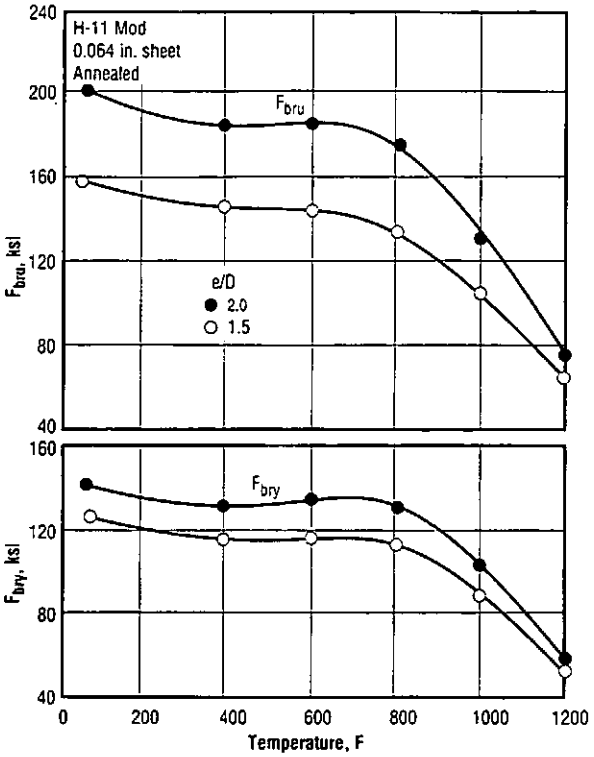

Fig. 3.3.6.1 Effect of test temperature on bearing properties of annealed sheet (Ref. 34)

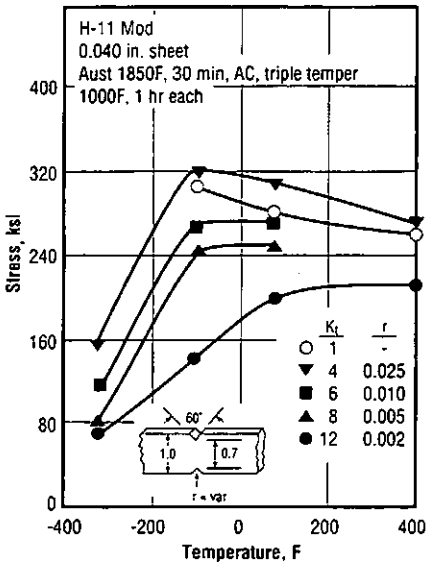

Fig. 3.3.7.1.1 Effect of test temperature on notch strength for various stress concentration factors of sheet (Ref. 15)

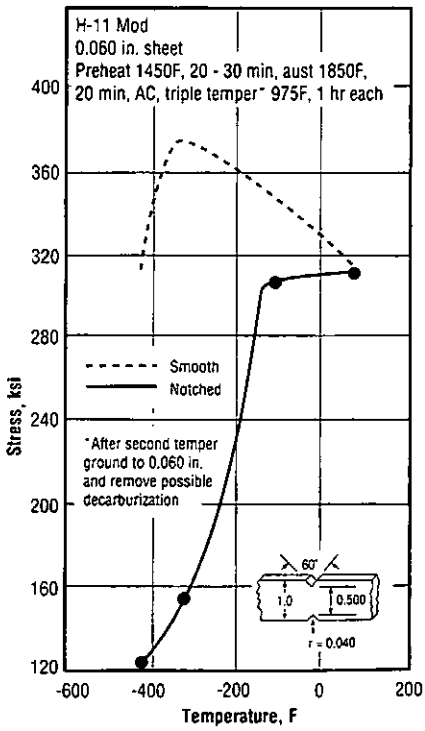

Fig. 3.3.7.1.2 Effect of low test temperature on notch strength of sheet (Ref. 26)

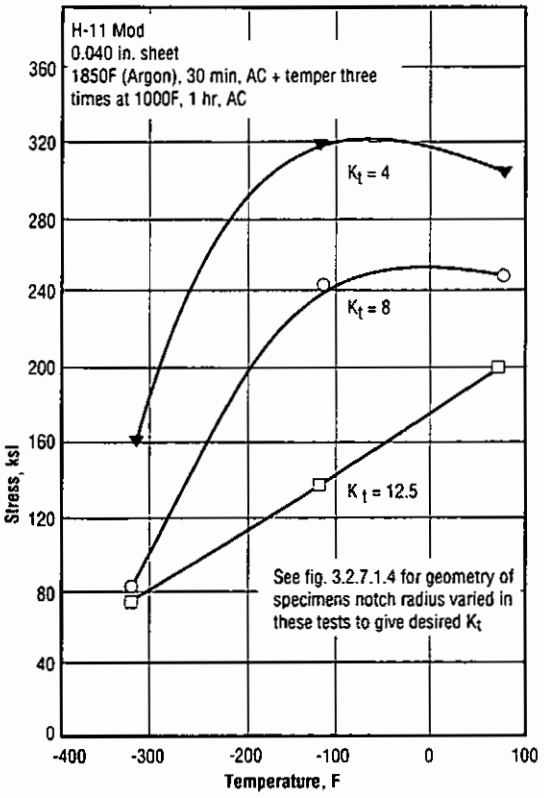

Fig. 3.3.7.1.3 Effect of low test temperature on notch tensile strength for stress concentration factors from 4 to 12.5 (Ref. 15)

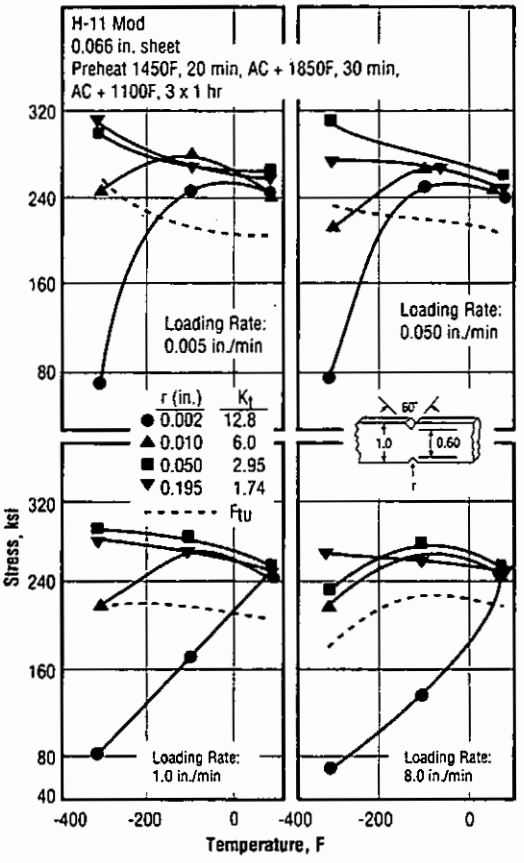

Fig. 3.3.7.1.4 Effect of low temperatures, loading rates and stress concentration factors on notch strength of sheet (Ref. 29)

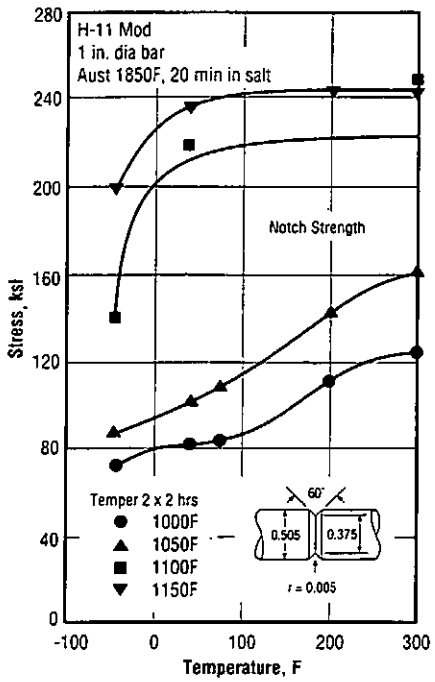

Fig. 3.3.7.1.5 Effect of low test temperature and tempering temperature on notch strength of bar (Ref. 30)

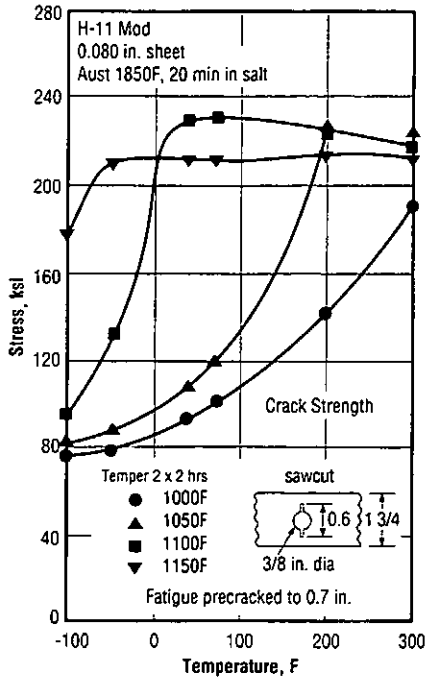

Fig. 3.3.7.1.6 Effect of low test temperature on crack strength of sheet (Ref. 30)

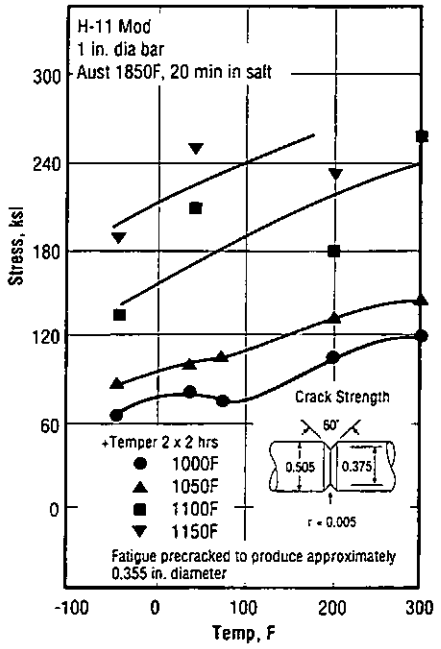

Fig. 3.3.7.1.7 Effect of low test temperature and tempering temperature on crack strength of bar (Ref. 30)

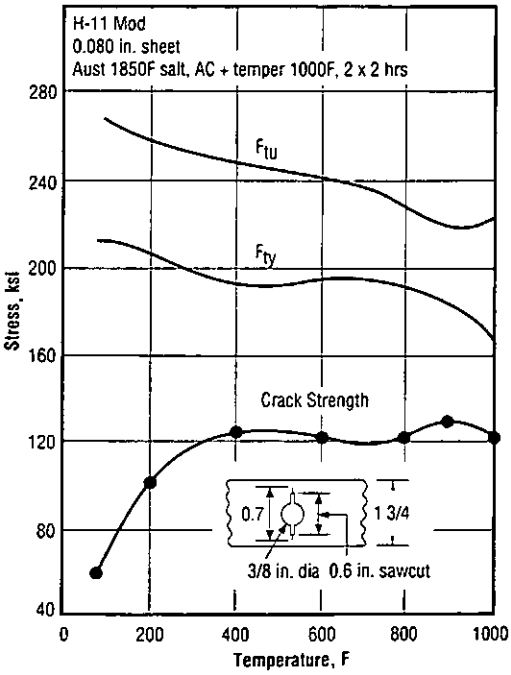

Fig. 3.3.7.1.8 Effect of test temperature on crack strength of sheet (Ref. 35)

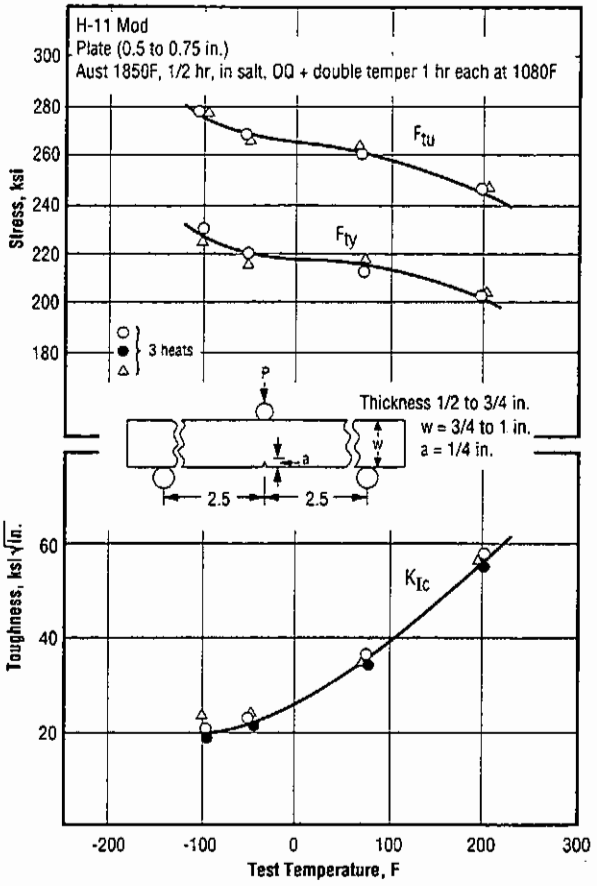

Fig. 3.3.7.2.1 Effect of test temperature on smooth specimen tensile properties and on fracture toughness of plate (Ref. 42)

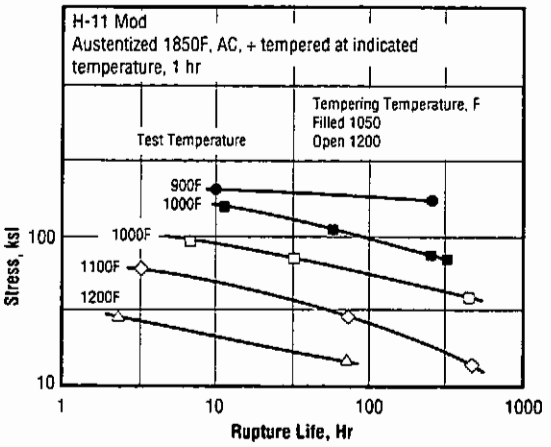

Fig. 3.4.1 Creep rupture behavior at 900 to 1200F for two tempering temperatures (Ref. 81)

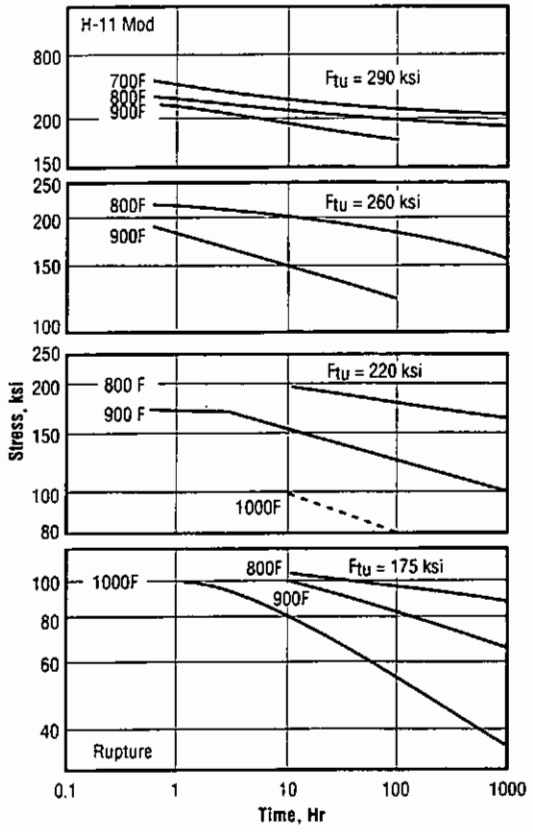

Fig. 3.4.2 Creep rupture curves for alloy at various strength levels at 700 to 1000F (Ref. 8)

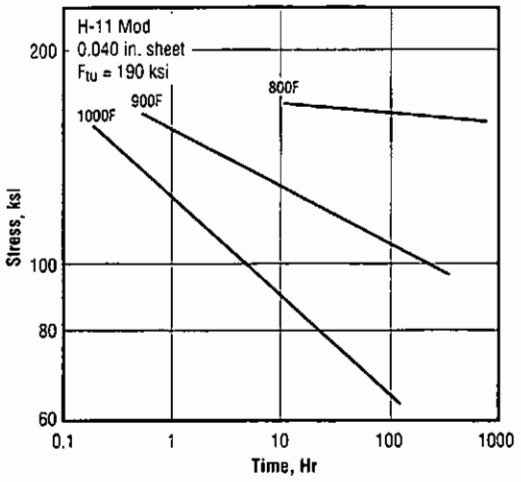

Fig. 3.4.3 Creep rupture curves at 800 to 1000F for sheet heat treated to F_{tu} = 190 ksi (Ref. 8)

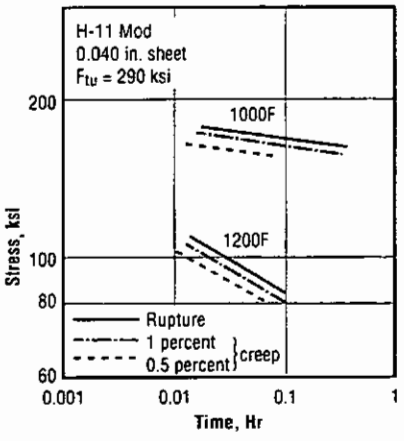

Fig. 3.4.4 Short time creep and creep rupture curves at 1000 and 1200F for sheet heat treated to F_{tu} = 290 ksi (Ref. 20)

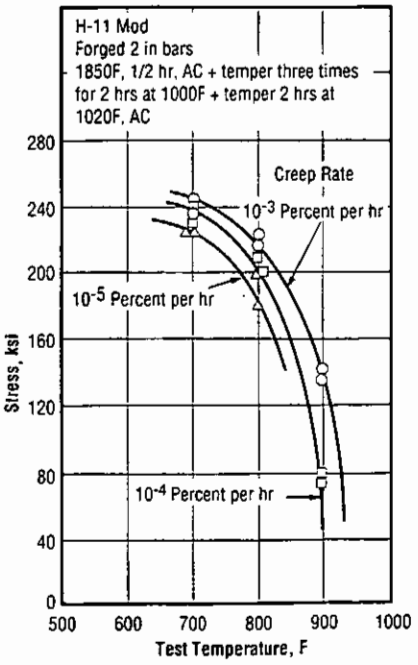

Fig. 3.4.5 Stress to produce creep rates of 10^{-3} to 10^{-5} percent per hr at 700 to 900F (Ref. 44)

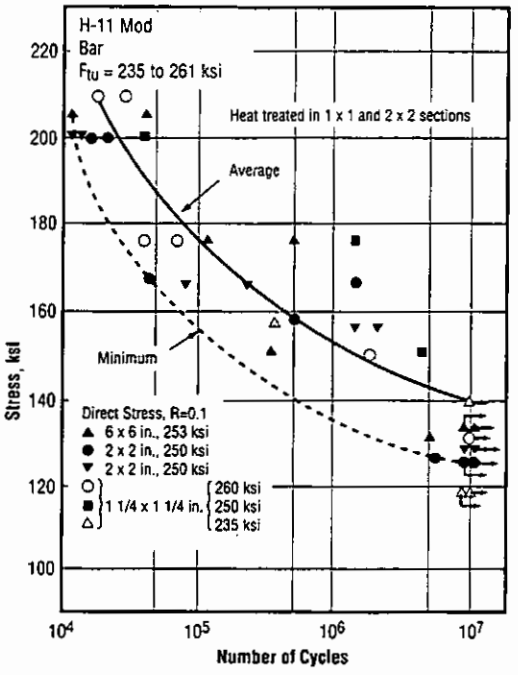

Fig. 3.5.1.1 S-N curves for heat treated bar (Ref. 12)

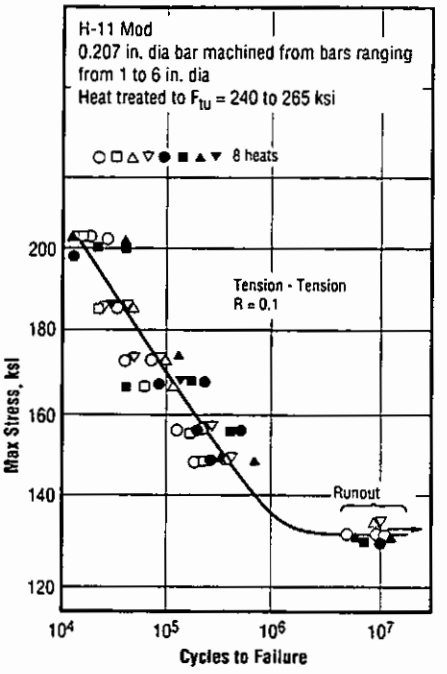

Fig. 3.5.1.2 Fatigue scatter band for bar specimens from eight separate heats tested in axial tension (Ref. 61)

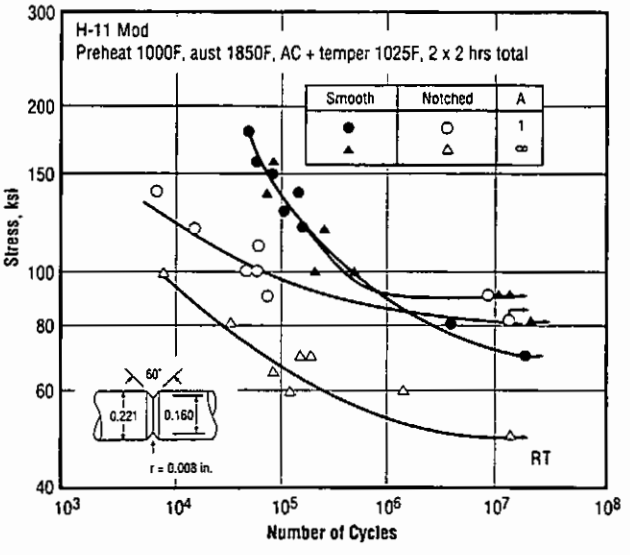

Fig. 3.5.1.3 S-N curves for notched and smooth specimens at room temperature (Ref. 28)

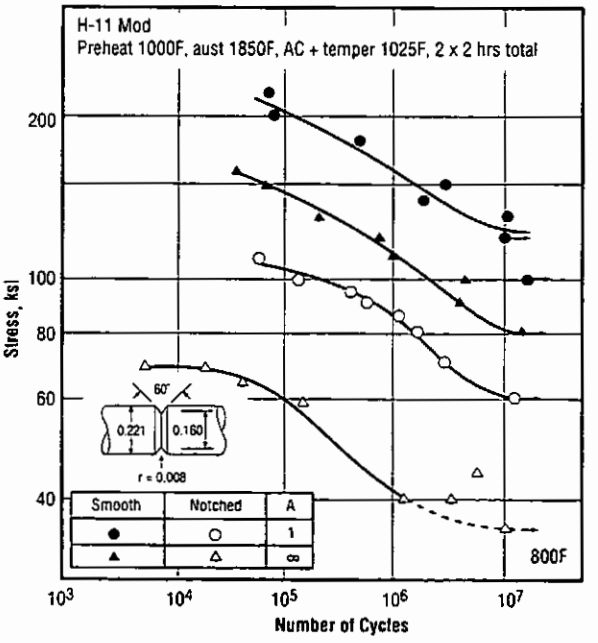

Fig. 3.5.1.4 S-N curves for notched and smooth specimens at 800F (Ref. 28)

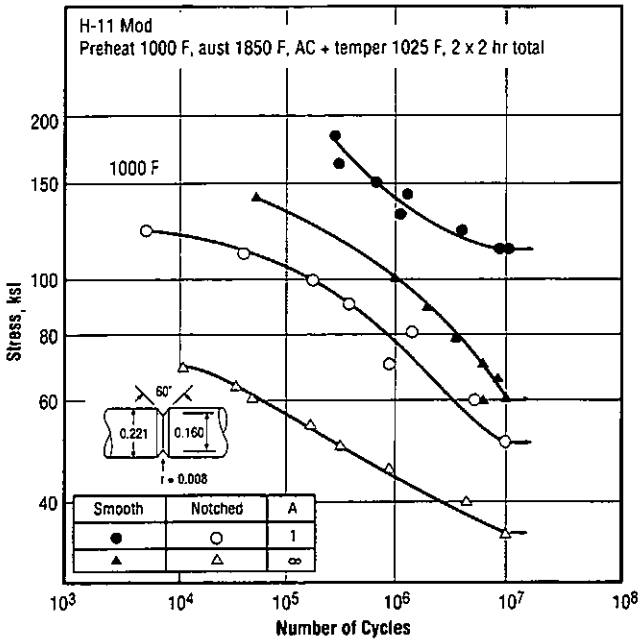

Fig. 3.5.1.5 S - N curves for notched and smooth specimens at 1000 F (Ref. 28)

Table 3.5.1.6 Fatigue properties of bar and bolts (Refs. 6-10, 12)

Alloy: H-11 Mod									
Form	**Bar**								
Condition	**Heat treated to F_{tu} = 260 ksi**								
Temp (F)	**Source**	**Method**	**Stress Ratio**		**Stress Concentration**	**Fatigue Strength (ksi) at Cycles**			
			A	**R**		**10^5**	**10^6**	**10^7**	**10^8**
RT	(7)	Rot bend	∞	-1	Smooth K_t=1	155	135	130	130
RT	(6)	Direct stress	0.82	0.1		155	135	130	130
	(10)					173	150	140	-
900	(6)					95	82	80	-
RT (a)	(6)					100	60	53	-
Form	**Threaded bolts**								
Condition	**Heat treated to F_{tu} = 260 ksi**								
Temp (F)	**Dia (in.) (b)**	**Method**	**Stress Ratio**		**Stress Concentration**	**Fatigue Strength (ksi) at Cycles**			
			A	**R**		**10^5**	**10^6**	**10^7**	**10^8**
RT	3/8	Direct stress	0.82	0.1		112	84	80	-
	1/2					118	94	90	-
900	3/8					91	81	80	-
RT (a)	3/8					95	60	55	-

(a) Tested at RT after exposure at 900F, 100 hr.
(b) Bolt types 3/8 in., 24 EWB: 1/2 in., 20 EWB.

Table 3.5.1.7 Tensile and fatigue properties at room temperature and at -320F for bolts machined from bar heat treated to 240 ksi yield strength (Ref. 60)

Alloy: H-11 Mod		
Form	**Smooth bar and 1/2 x 20 aircraft bolt**	
Condition	**Unspecified heat treatment to obtain tensile properties shown**	
Test temp.	**70F**	**-320F**
Material F_{tu} (ksi)	279	302
Material F_{ty} (ksi)	240	263
e, 4D (percent)	11.5	10.2
RA (percent)	42	39
Charpy impact (a) (ft lbs)	5	1.5
Bolt F_{tu} (ksi)	280	297
Bolt, fatigue cycles at 135 ksi max. stress, R = 0	100,000	65,000

(a) Subsize specimen per ASTM E 23, Type W.

Table 3.5.1.8 Tensile and fatigue properties of bolts made from material heat treated to several strength levels (Ref. 60)

Alloy: H-11 Mod			
Form	**Smooth bar and 1/2 x 20 aircraft bolt**		
Condition	**Unspecified heat treatments to obtain tensile properties shown**		
	A	**B**	**C**
Material F_{tu} (ksi)	197.7	236.8	288
Material F_{ty} (ksi)	158.2	199.4	243.7
e, 4D (percent)	15.5	13.5	12.1
RA (percent)	47.7	48.3	41.4
Notch ratio at K_t = 6	1.4	1.3	1.1
Bolt F_{tu} (ksi)	198	239	288.4
Fatigue cycles at max. stress approx. 1/2 F_{tu} (a), R = 0	321,100	417,600	700,000

(a) 93 ksi for A, 115 ksi for B, 135 ksi for C.

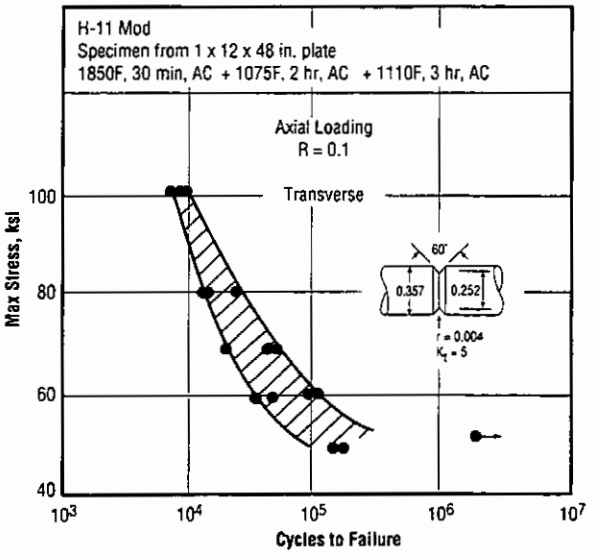

Fig. 3.5.1.9 Low cycle fatigue of notched (K_t = 5.0) specimens cut from large place. (Ref. 70)

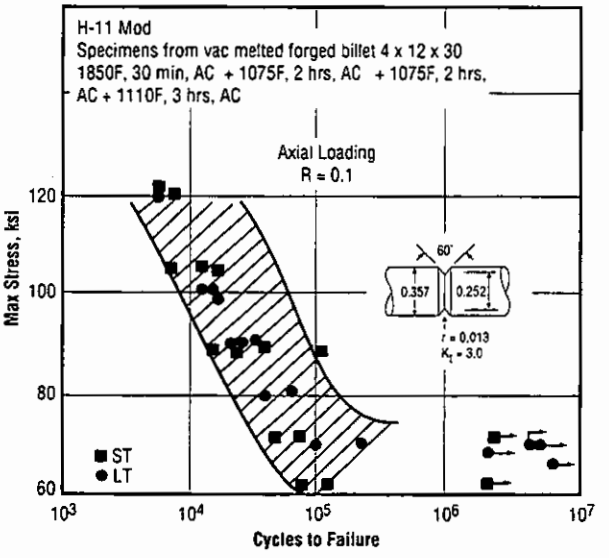

Fig. 3.5.1.10 Low-cycle fatigue of notched (K_t = 3.0) specimens cut from long and short transverse directions of forging (Ref. 70)

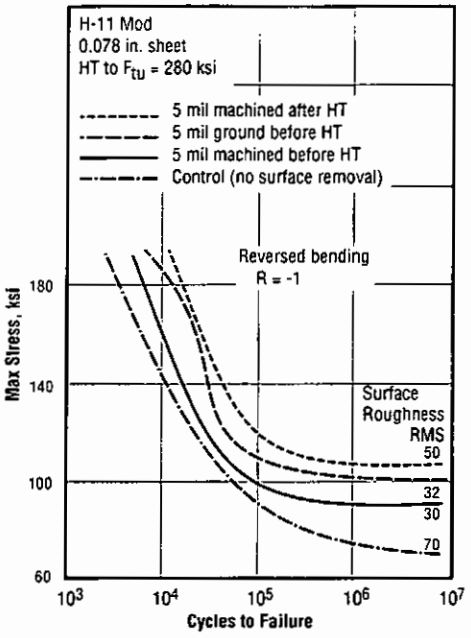

Fig. 3.5.1.11 Effect of surface machining and grinding (to remove decarburized layer) on reversed bending fatigue of sheet (Ref. 72)

Table 3.5.1.12 Fatigue strength at 10^6 cycles in rotating bending for vacuum and air melted alloy in various conditions of surface treatment after exposure to elevated temperature (Ref. 39)

Alloy: H-11 Mod							
Form	**Rot. beam spec. from 6 in. square air melt or CVM billet**						
Condition (a)	**CVM: F_{tu} = 272 ksi, F_{ty} = 228 ksi, e = 7 percent Air Melt: F_{tu} = 264 ksi, F_{ty} = 222 ksi, e = 7 percent**						
	10^6 cycle. Endurance limits (ksi) at 75F after 4 hr exposure at temperature indicated						
		75F	**375F**	**500F**	**750F**	**1000F**	**1250F**
Polished	Air	91	91	88	85	81	64
	Vac	94	93	90	90	90	80
Cr plated (0.002 in.)	Air	54	-	-	74	80	-
	Vac	56	60	63	80	87	-
Peened (b)	Air	90	87	-	-	82	66
	Vac	96	94	90	89	89	80
Plated & Peened	Air	89	88	87	83	76	72
	Vac	96	94	90	89	88	80
Peened & Plated	Vac	96	-	-	-	87	-

(a) 1850F, 45 min, AC, + double temper 1050F, 2 hr, AC.
(b) .009 to .010A (on Almen Scale, refers to height of arc of standard strip specimen after being subjected to similar peening on one side only).

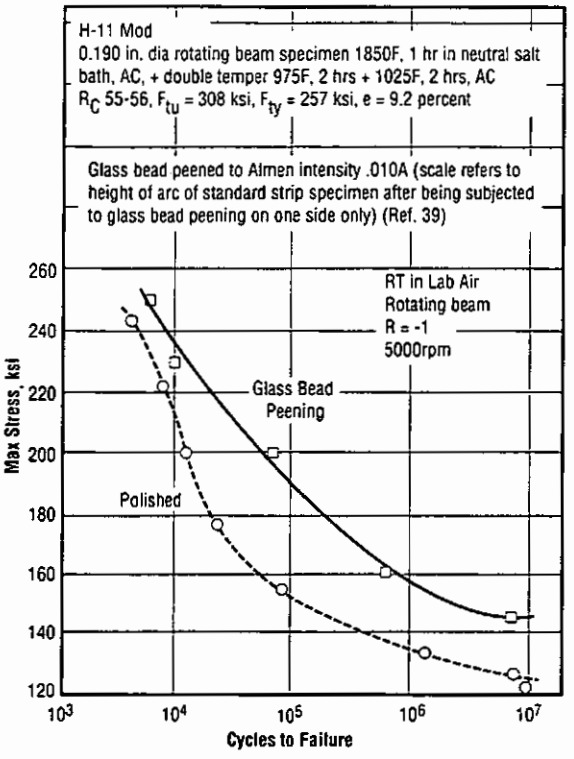

Fig. 3.5.1.13 S-N curves in rotating beam bending for smooth specimens and for specimens subjected to glass bead peening (Ref. 39)

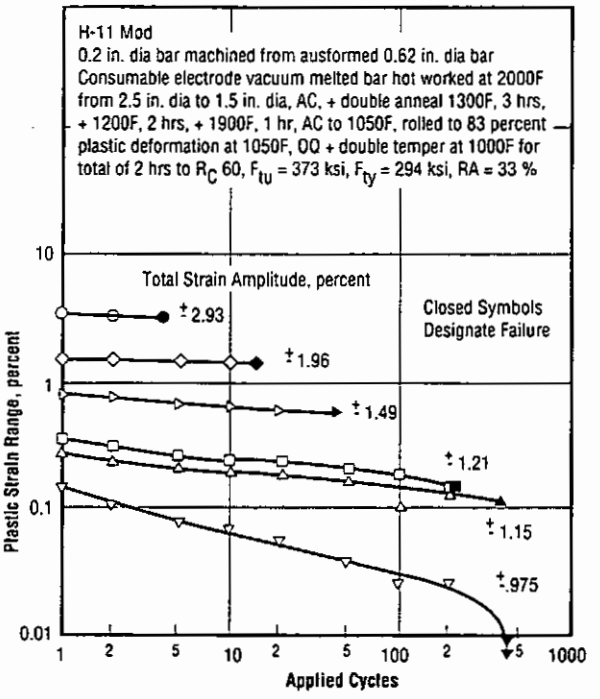

Fig. 3.5.1.14 Cyclic strain hardening in ausformed bar as manifested by reduction in plastic strain range (increase in elastic strain range) as cycles are increased during strain cycling tests in which total strain amplitudes are maintained constant (Ref. 64)

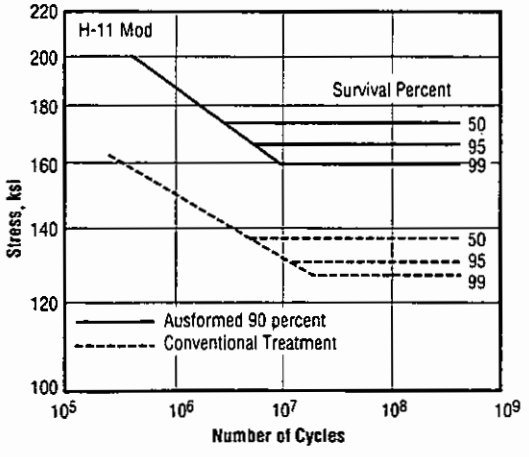

Fig. 3.5.1.15 S-N curves for ausformed and conventionally heat treated steel (Ref. 37)

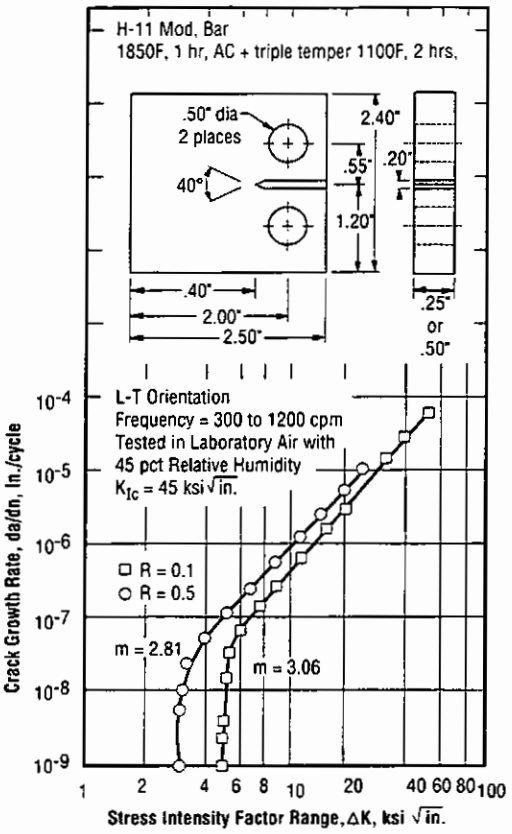

Fig. 3.5.2.2 Fatigue crack growth rates in air at room temperature (Ref. 97)

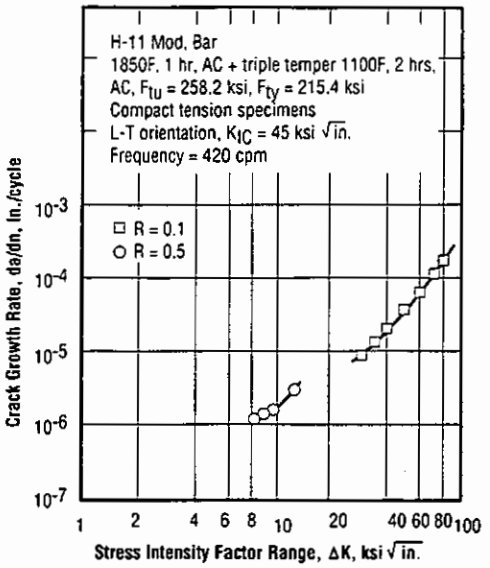

Fig. 3.5.2.3 Fatigue crack growth rates in air at 650F (Ref. 100)

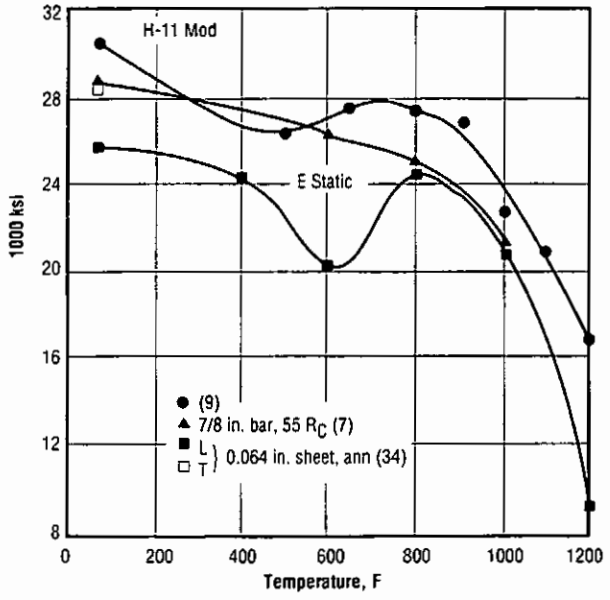

Fig. 3.6.2.1 Modulus of elasticity at room and elevated temperatures (Refs. 7, 9, 34)

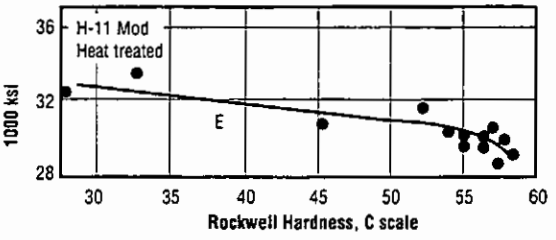

Fig. 3.6.2.2 Modulus of elasticity for alloy heat treated to various hardness levels (Ref. 9)

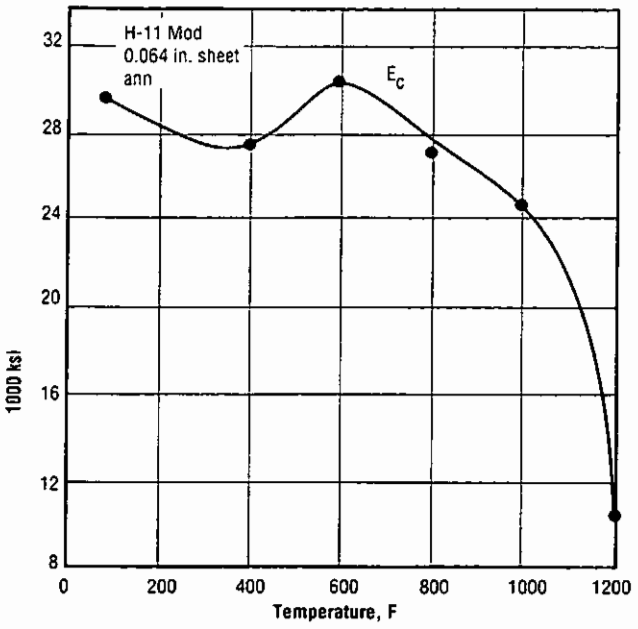

Fig. 3.6.2.3 Modulus of elasticity in compression at room and elevated temperatures for annealed sheet (Ref. 34)

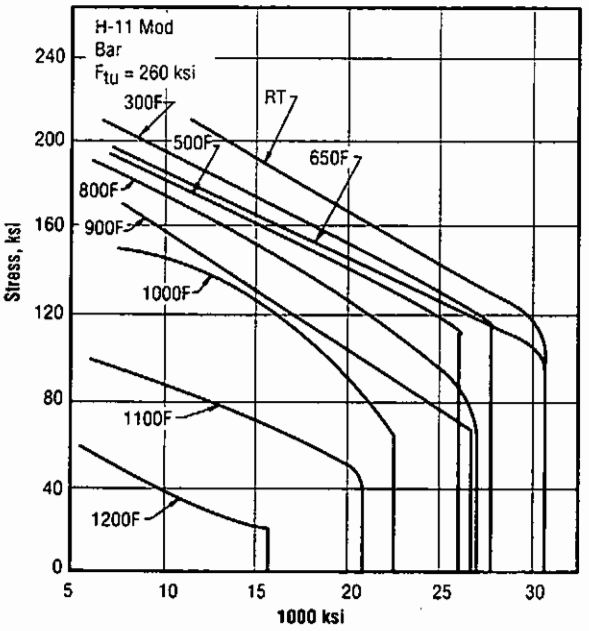

Fig. 3.6.4.1 Tangent modulus curves at room and elevated temperatures for bar heat treated to F_{tu} = 260 ksi (Ref. 11)

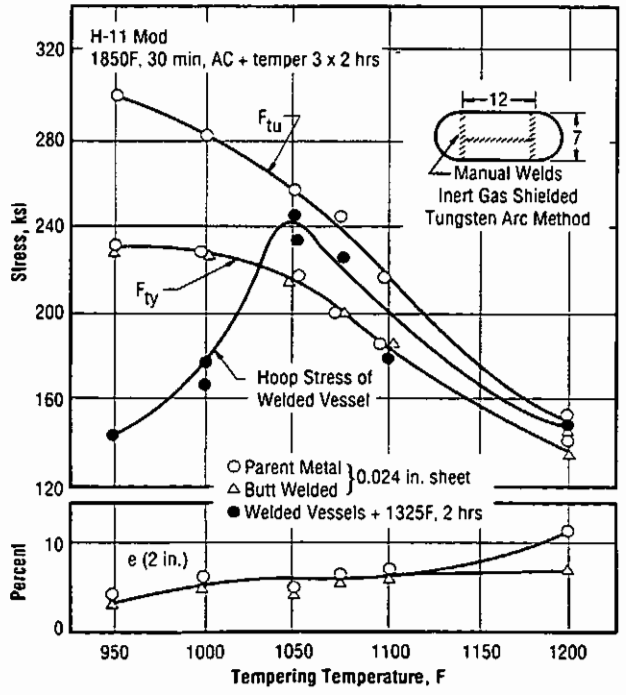

Fig. 4.3.2 Effect of tempering temperature on strength of welded sheet and pressure vessels (Ref. 21)

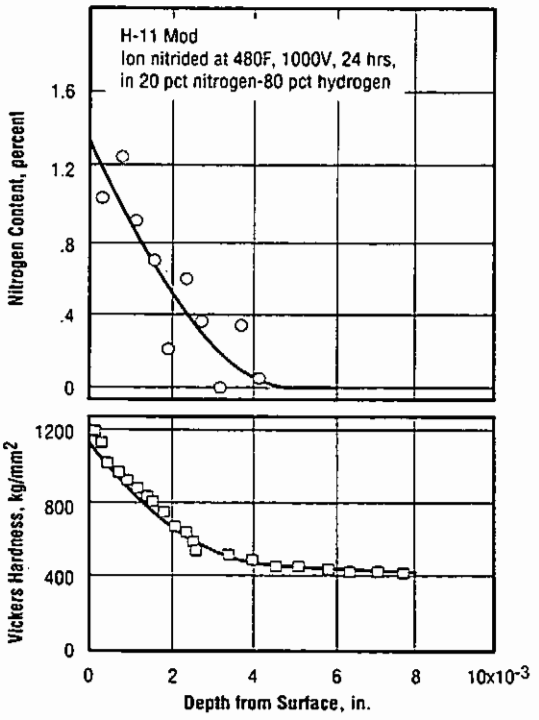

Fig. 4.4.5 Nitrogen content and hardness profiles for ion-nitrided H-11 Mod (Ref. 99)

References

1. AMS 6437A (January 31, 1964; replaced by Ref. 77).
2. AMS 6485B (May 1, 1969; replaced by Ref. 78).
3. AMS 6487C (May 1, 1968; replaced by Ref. 79).
4. North American Aviation, Inc., Columbus Div., "Thermold A, Thermold J and Vascojet 1000 Steel Sheet Evalution," Rep. No. NA 58H-302 (July 22, 1958).
5. North American Aviation, Inc., Columbus Div., "Thermold J and Vascojet 1000 Bar and Billet Evalution," Rep. No. NA 58 H-416 (October 9, 1958).
6. Vanadium Alloys Steel Co., "Inspection Results on Vascojet 1000 Billets for North American Aviation," Data Sheet (September 1959).
7. Allegheny Ludlum Steel Corp., "AISI H 11 or Potomac A," Data Sheet (September 1959).
8. Crucible Steel Co. of America, "Crucible 218, Martensitic Type High Temperature Steel" (May 1958).
9. Vanadium Alloys Steel Co., "Vascojet 1000 for Ultra High Strength Structural Requirements" (1959).
10. Baumgartner, T., Standard Pressed Steel Co., Rep. No. 86 (May 1957).
11. Vanadium Alloys Steel Co., "Mechanical and Physical Properties of Vascojet 1000," Data Sheet (November 4, 1958).
12. Boder, N., and Simkovich, E. A., "Tension-Tension Fatigue Properties of 5Cr-Mo-V Steel Bar Heat Treated to the 220 - 270 ksi Ultimate Tensile Strength Range," Republic Aviation Corp., ERMR 387G (May 19, 1958).
13. Espey, G. B.; Jones, M. H.; and Brown, W. F., Jr., "The Sharp Edge Notch Tensile Strengths of Several High-Strength Steel Sheet Alloys," *Proceedings* of the ASTM, Vol. 59 (1959).
14. Srawley, J. E., and Beachem, C. D., "Crack Propagation Tests of Some High Strength Sheet Steels," NRL Rep. 5263 (January 10, 1959).
15. Sachs, G., and Sessler, J. G., "Effect of Stress Concentration on Tensile Strength of Titanium and Steel Alloy Sheet at Various Temperatures," ASTM, STP No. 287 (1960).
16. Cameron Iron Works, Inc., Houston, TX, "Report on Evaluation of the Forgeability and Mechanical Properties of Vascojet 1000 Alloy," Project ZAX-14, ZCLR-154 (1958).
17. Shannon, J. L., Jr.; Espey, G. B.; Repko, A. J.; and Brown, W. F., Jr., "Effect of Carbon Content and Melting Practice on Room Temperature Sharp Edge Notch Tensile Characteristics of H-11 Modified and 300M Sheet Steels," *Proceedings* of the ASTM, Vol. 60 (1960).
18. AiResearch (1958).
19. Cleveland Pneumatic Tool Co. (1958).
20. International Nickel Co. (1958).
21. Baloga, M., "Effect of Heat Treatment Variations on the Bursting Strength of Thin Walled Pressure Vessels Fabricated from Vascojet 1000 Steel," Martin Co., Rep. No. ER-10121-5 (September 1958).
22. Hamaker, J. E., Jr., and Vater, E. J., "Carbon Strength Relationships on 5 Percent Chromium Ultra High Strength Steels," *Proceedings* of the ASTM, Vol. 60 (1960).
23. American Iron and Steel Institute, "High Temperature High Strength Alloys" (February 1963).
24. Crucible Steel Company, "Halcomb 218 Hot Work Steel," Data Sheet No. 4 (October 1962).
25. Adams, J. G., "The Determination of Spectral Emissivities Reflectivities and Absorptivities of Materials and Coatings," Northrop Corporation Report No. Nor. 61-189 (August 3, 1961).
26. Rice, L. P.; Cambell, J. E.; and Simmons, W. F., "Evaluation of the Effects of Very Low Temperature on Properties of Aircraft and Missile Metals," WADD TR 60-214 (February 1960).
27. "Fracture Testing of High Strength Sheet Materials," 3rd Report of a Special ASTM Committee Materials Research and Standards, Vol. 1 (November 1961).
28. Brodrick, R. F., "Fatigue and Dynamic Creep of High Strength Steels," ASD TDR-62-480 (August 1962).
29. Brisbane, A. W., "The Investigation of the Effects of Loading Rate and Stress Concentration Factors on the Notch Properties of Three Sheet Alloys at Subzero Temperatures," ASD TDR-62-930 (March 1963).
30. Hanna, G. L., and Steigerwald, E. A., "Fracture Characteristics of Structural Metals," Final Summary Technical Report ER-5426, TAPCO Division Thompson Ramo Wooldridge, Inc. (June 30, 1963).
31. Martin, C. F.; Gerberich, W. W.; McCamont, J. M.; and Harmon, K. L., "Research in the Mechanism of Strengthening in Ausformed Steel," ASD TDR-62-692 (February 1963).
32. Semka, R. P.; Heise, R. E.; and Ross, S. T., "Ausform Processing of Steel by Forging," ASD TR-61-428 (March 1962).
33. Banerjee, B. R., and Hauser, J. J., "Research and Application Engineering to Determine the Effect of Processing Variables in Crack Propagation of High-Strength Steels and Titanium," ASD TDR-62-1034, Part 1 (April 1963).
34. Henning, R. G., and Brisbane, A. W., "Mechanical Properties of AM 350, Potomac A, Potomac M, and Vasco Jet-1000 Steel Alloys in the Annealed Condition," ASD TDR-63-116 (May 1963).
35. Steigerwald, E. A., and Hanna, G. L., "Strain Aging and Delayed Failure in High-Strength Steels," ASD TDR-62-968 (November 1962).
36. Yount, R. E., "Determination of Engineering Propertiesof Mar-Strained Steels," ASD TDR-62-230 (August 1962).

37. Justusson, W. M., and Zackay, V. W., "Engineering Properties of Ausformed Steel," *Metal Progress*, Vol. 82, No. 6 (December 1962).

38. Allegheny Ludlum Steel Corp., "Potomac A, Hot Work and Structural Steel AISI Type H-11" (1972).

39. Campbell, J. E., "Shot Peening for Improved Fatigue Properties and Stress-Corrosion Resistance," MCIC Report 71-02 (December 1971).

40. Bucher, J. H.; Powell, G. W.; and Spretnak, J. W., "A Micrographic Analysis of Fracture Surfaces in Some Ultra-High-Strength Steels," in *Application of Fracture Toughness Parameters to Structural Metals*, H. D. Greenberg, ed., AIME Metallurgical Soc. Conf., Vol. 31 (1966).

41. Johnson, H. H., and Willner, A. M., "Moisture and Stable Crack Growth in a High Strength Steel," *Applied Materials Research*, pp. 34-40 (January 1965).

42. Steigerwald, E. A., "Plane Strain Fracture Toughness for Handbook Presentation," AFML-TR-67-187 (July 1967).

43. Chait, R., "Factors Influencing the Strength Differential in High Strength Steels," *Met. Trans.*, Vol. 3, pp. 365-371 (February 1972).

44. VanEcho, J. A., and Simmons, W. F., "Supplemental Report on the Elevated Temperature Properties of Chromium-Molybdenum Steels," ASTM Data Series Publication No. DS 6S1 (June 1966).

45. Carman, C. M., and Katlin, J. M., "Low Cycle Fatigue Crack Propagation Characteristics of High Strength Steels," *Trans. ASME Jour. Basic Eng.*, Paper No. 66-Met 3 (1966).

46. Walter, R. J., and Chandler, W. T., "Effects of High-Pressure Hydrogen on Metals at Ambient Temperature," Final Report to NASA on Contract NAS8-19, Rocketdyne Report R-7780-2 (February 28, 1969).

47. Freedman, A. H., "An Accelerated Stress Corrosion Test for High Strength Ferrous Alloys," *Jour. of Materials*, Vol. 5, No. 2, pp. 431-166 (June 1970).

48. Beck, W., and Jankowsky, E. J., "Delayed Brittle Failure in Cadmium Plated Steels," *Metal Progress*, pp. 92-95 (August 1963).

49. Kalish, D.; Kulen, S. A.; and Cohn, M., "Thermomechanical Treatments Applied to Ultra High Strength Bainites," *Structure and Properties of Ultra High Strength Steels*, ASTM STP 370, pp. 172-207 (March 1965).

50. Humphries, T. S., and Nelson, E. E., "Stress Corrosion Cracking Evaluation of Several Ferrous and Nickel Alloys," NASA TMX-64511 (April 2, 1970).

51. Amateau, M. F., and Steigerwald, E. A., "Fracture Mechanics of Structural Metals," Final Report to U.S. Navy Bureau of Naval Weapons Contract NOw-64-0186 C Report No. ER 5937-3 (January 22, 1965).

52. Carter, C. S., "Stress Corrosion Crack Branching in High Strength Steels," *Engineering Fracture Mechanics*, Vol. 3, No. 1, pp. 1-14 (July 1971).

53. Wei, R. P., and Landes, J. D., "Correlation Between Sustained-Load and Fatigue Crack Growth in High-Strength Steels," ASTM MRS Vol. 9, No. 7, pp. 25-28 (July 1969).

54. Miller, G. A., "The Dependence of Fatigue Crack Growth Rate on Stress Intensity Factor and the Mechanical Properties of Some High-Strength Steels," *Trans. ASM*, Vol. 61, pp. 442-447 (1968).

55. Bert, C. W.; Mills, E. J.; and Hyler, W. J., "Mechanical Properties of Aerospace Structural Alloys Under Biaxial Conditions," AFML TR 66-229 (August 1966).

56. Benjamin, W. D., and Steigerwald, E. A., "Environmentally Induced Delayed Failures in Martensitic High Strength Steels," AFML-TR-68-80 (April 1968).

57. Groenveld, T. P.; Fletcher, E. E.; and Elsea, A. R., "A Study of Hydrogen Embrittlement of Various Alloys," Final Report of NASA, G. C. Marshall Space Flight Center, Contract NAS8-20029 (1969).

58. Manning, G. K., "Effect of Small Crack on the Load Carrying Ability of High Strength Steel," in "Evaluation of Metallic Materials in Design for Low-Temperature Service," ASTM STP 302, pp. 49-68 (1961).

59. Schaeffer, G. T., and Weiss, V., "Effect of Section Size on Notch Tensile Strength," Interim Tech. Report No. 2, University of Syracuse to Army Research Office Durham, Contract DA-31-124-ARO (D)-106 (June 1964).

60. Hood, A. C., and Sproat, R. L., "Ultra High Strength Steel Fasteners," ASTM STP 370, pp. 208-221 (1965).

61. Simkovich, E. A., and Loria, E. A., "Effect of Decarburization and Grinding Conditions on Fatigue Strength of 5 Percent Cr-Mo-V Sheet Steel," ASM Preprint No. 185 (October 17-21, 1960).

62. Jones, R. L., and Nordquist, F. C., "An Evaluation of High Strength Steel Forgings," RTD-TDR-63-4050 (May 1964).

63. Dreyer, G. A., and Gallaugher, W. C., "Investigation of the Effects of Stress Corrosion on High Strength Steel Alloys," A. F. Mat. Lab., ML-TDR-64-3 (February 1964).

64. Matheny, J. E., Jr., "Low Cycle Fatigue Properties of the Ausformed Steel," University of Illinois, T & A. M. Report No. 308 (February 1968).

65. Kendall, D. P., and Davidson, T. E., "The Effect of Strain Rate on Yielding of High Strength Steels," Watervliet Arsenal Report WVT 6618 (May 1966).

66. Kendall, D. P., "The Effect of Strain Rate and Temperature on Yielding in Steels," Watervliet Arsenal Report WVT 7061 (November 1970).

67. Warren, K. A., and Reed, R. P., "Tensile and Impact Properties of Selected Materials From 20 to 300°K," NBS Monograph 63 (June 28, 1963).

68. Hamaker, J. C., Jr., and Vater, E. J., "Carbon: Strength Relationships in 5 Percent Chromium Ultra-High Strength Steels," Preprint 800, ASTM (1960).

69. Gerberich, W. W.; Williams, A. J.; Martin, C. F.; and Heise, R. E., "Ausform Fabrication and Properties of High Strength Alloy Steel," ASTM STP 370, pp. 154-171 (1965).

70. Pratt, W. M., "Material Evaluation of H-11 High Strength Steel for F-111," General Dynamics, Fort Worth, Report N64-20060 (April 15, 1964).

71. Hanna, G. L., and Steigerwald, E. A., "Influence of Environment on Crack Propagation and Delayed Failures in High Strength Steels," A. F. Mat. Lab. Report No. RTD-TDR-63-4225 (January 1964).

72. Ruff, P. E., "Hot Work Tool Steel for Aircraft," *Metal Progress*, Vol. 75, pp. 103-107 (March 1959).

73. AMS 6488A (May 15, 1971) [See Ref. 80].

74. Banerjee, B. R., "Fracture Micromechanics in High Strength Steels," ASTM STP 370, pp. 94-120 (March 1965).

75. Kueser, P. E., "Magnetic Materials Topical Report," NASA CR 54091, Westinghouse WAED 6452E (September 1964).

76. Ketcham, S. J., "Chemical Milling of Alloy Steels," Report No. NAEC-AML-2418, U.S. Naval Air Engineering Center (March 1966).

77. AMS 6437D, Society of Automotive Engineers (Oct. 1985).

78. AMS 6485F, Society of Automotive Engineers (July 1, 1989).

79. AMS 6487F, Society of Automotive Engineers (January 1, 1990).

80. AMS 6488D, Society of Automotive Engineers (January 1, 1985).

81. Philip, T. V., and McCaffrey, T. J., "Ultrahigh-Strength Steels," 1990 Metals Handbook, 10th Ed., Vol. 1, ASM Int'l. Materials Park, OH, *Properties and Selection: Iron, Steels, and High-Performance Alloys*, pp. 430-448.

82. "Chromo-V," *Alloy Digest*, Filing Code TS-313 (February 1977).

83. "Carpenter No. 882," *Alloy Digest*, Filing Code TS-339 (October 1978).

84. "Hotform No. 2," *Alloy Digest*, Filing Code TS-394 (February 1982).

85. "Guterl H-11," *Alloy Digest*, Filing Code TS-412 (March 1983).

86. "AL Tech Potomac A," *Alloy Digest*, Filing Code TS-478 (July 1987).

87. Umemoto, M.; Ohtsuka, H.; and Tamura, I., "Transformation to Pearlite from Work-Hardened Austenite," Transactions of the Iron and Steel Institute of Japan, Vol. 23:9 (Sept. 83).

88. Kerns, G. E.; Wang, M. T.; and Staehle, R. W., "Stress Corrosion Cracking and Hydrogen Embrittlement in High Strength Steels," *Proceedings* of an Int'l. Corrosion Conference in France, pp. 700-735 (June 12-16, 1973).

89. Kroupa, K. M.; Venkatesan, P. S.; and Wood, J. D., "Fracture Toughness of H-11 Steel and Its Susceptibility to Stress Corrosion Cracking," *Engineering Fracture Mechanics*, Vol. 8, pp. 547-553 (1976).

90. Saia, R. J., and Gould, G. C., "Evaluating the Corrosivity of Manufacturing Chemicals," presented at ASME Conference on Improved Technology for Critical Bolting Applications, Chicago, IL (July 20-24, 1986).

91. Namboodhiri, T. K. G., "Measurement of Hydrogen in Metals," *Transactions of The Indian Institute of Metals*, Vol. 31, No. 6, pp. 435-438 (December 1978).

92. Powell, R. W.; Peterson, D. T.; Zimmerschied, M. K.; and Bates, J. F., "Swelling of Several Commercial Alloys Following High Fluence Neutron Irradiation," *Journal of Nuclear Materials*, Vol. 104, No. 1-3, pp. 969-973 (1981).

93. Ule, B.; Vodopivec, F.; Pristavec, M.; and Gresovnik, F., "Temper Embrittlement of Hot Work Die Steel," *Materials Science and Technology*, Vol. 6, No. 12, pp. 1181-1185 (December 1990).

94. Garrison, W. M., Jr., "Influence of Silicon on Strength and Toughness of 5 wt. Percent Chromium Secondary Hardening Steel," *Materials Science and Technology*, Vol. 3, No. 4, pp. 256-259 (April 1987).

95. Pacyna, J., "Effect of Non-Metallic Inclusions on Fracture Toughness of Tool Steels," *Steel Research*, Vol. 57, No. 11, pp. 586-592 (1986).

96. Place, T. A.; Howarth, R. A.; and Smith, N. L., "Microstructural Analysis of Toughness Anomalies in H-11 Steel," presented at ISTFA Conference on Testing and Failure Analysis, San Jose, CA (October 25-27, 1982).

97. Mackay, T. L.; Alperin, B. J.; and Bhatt, D. D., "Near-Threshold Fatigue Crack Propagation of Several High Strength Steels," *Engineering Fracture Mechanics*, Vol. 18, No. 2, pp. 403-416 (1983).

98. Pickering, F. B., "The Properties of Tool Steels for Mold and Die Applications," presented at Conference on Tool Materials for Molds and Dies: Application and Performance, St. Charles, IL (September 30-October 2, 1987).

99. Trejo-Luna, R.; Zironi, E. P.; Rickards, J.; and Romero, G., "Some Features of Low-Temperature Ion Nitriding of Steels," *Scripta Metallurgica*, Vol. 23, pp. 1493-1496 (1989).

100. Gallagher, J., "Damage Tolerant Design Handbook," Metals and Ceramics Information Center, Battelle-Columbus Laboratories, pp. 6.13-1 - 6.13-12, distributed by CINDAS/Purdue (1983).

101. AMS 2416G, "Plating, Nickel-Cadmium, Diffused," Society of Automotive Engineers (Oct. 1990).

This page is blank.